5 Driven Quantum Systems

Peter Hänggi

5.1 Introduction

During recent years we could bear witness to an immense research activity, both in experimental and theoretical physics, as well as in chemistry, aimed at understanding the detailed dynamics of quantum systems that are exposed to strong time-dependent external fields. The quantum mechanics of explicitly time-dependent Hamiltonians generates a variety of novel phenomena that are not accessible within ordinary stationary quantum mechanics. In particular, the development of laser and maser systems opened the doorway for creation of novel effects in atoms and molecules, which interact with strong electromagnetic fields [1–4]. For example, an atom exposed continuously to an oscillating field eventually ionizes, whatever the values of the (angular) frequency ω and the intensity I of the field is. The rate at which the atom ionizes depends on both, the driving frequency ω and the intensity I. Interestingly enough, in a pioneering paper by H. R. Reiss in 1970 [5], the seemingly paradoxical result was established that extremely strong field intensities lead to smaller transition probabilities than more modest intensities, i.e. one observes a declining yield with increasing intensity. This phenomenon of stabilization that is typical for the above threshold ionization (ATI) is still actively discussed, both in experimental and theoretical groups [6, 7]. Other activities that are in the limelight of current topical research relate to the active control of quantum processes; e.g. the selective control of reaction yields of products in chemical reactions by use of a sequence of properly designed coherent light pulses [8].

Our prime concern here will focus on the quantum dynamics of driven bistable systems. Such systems exhibit an interplay of three characteristic components, (i) nonlinearity, (ii) nonequilibrium behaviour (as a result of the driving), and (iii) quantum tunneling, with the latter providing a paradigm for quantum coherence phenomena.

We shall approach this complexity of driven quantum systems in a sequence of steps. In Sect. 5.2 we introduce archetypal time-dependent interaction schemes such as the dipole interaction with laser fields or the electron spin resonance system. Section 5.3 introduces the reader to a variety of tools suitable for tackling the quantum dynamics of explicitly time-dependent (time-periodic and non-periodic) Schrödinger equations. Exactly solvable quantum systems with time-dependent potentials are dis-

cussed in Sect. 5.4. Among these are the quantum mechanics of a two-level system (TLS) interacting with a circularly polarized laser field. Clearly, the presence of so-called anti-rotating terms makes most systems inaccessible to analytical closed solutions. Hence, we address with Sect. 5.5 prominent numerical methods for periodically driven quantum systems. As an application to driven quantum systems, we study in Sect. 5.6 the phenomenon of coherent tunneling in periodically driven bistable quantum systems. As an intriguing result, we demonstrate therein that an appropriately designed coherent conyinuous-wave (cw) driving can bring quantum tunneling to an almost complete standstill (coherent destruction of tunneling [9]). This phenomenon in turn produces other novel quantum phenomena such as low-frequency radiation and/or intense, non-perturbative, even-harmonic generation in symmetric systems that possess an inversion symmetry [10]. The possibility of controlling quantum dynamics by application of shape- and phase-designed pulse perturbations is elucidated in Sect. 5.7 with a time-dependent dipole coupling between two Born-Oppenheimer surfaces. Conclusions and an outlook are given in the final Sect. 5.8.

5.2 Time-dependent interactions

It is a well-known fact that the time evolution of an isolated quantum system, described by a Hamiltonian H_0 with a discrete spectrum that acts on the space of relevant system variables $\boldsymbol{x}$ cannot exhibit the type of behaviour usually associated with deterministic chaos of classical systems. This is so because the time evolution of a quantum state is almost periodic since it can be expanded in terms of the eigenfunctions ψ_n with eigenvalues E_n. Only when the spacing between energy levels becomes very small, the quantum system can imitate various features of the classical behaviour on certain time scales. It should be noted, however, that even very small quantum systems such as atoms, quantum dots, molecules, etc., can exhibit a nontrivial behaviour when exposed to intense external fields. Some typical situations are introduced in the following subsections.

5.2.1 Laser interactions

A vast variety of new nonlinear phenomena such as above-threshold ionization of atoms, multi-photon dissociation or excitation of atoms or molecules occur in intense laser fields [1–7]. Usually, the relevant wavelength of the radiation field is far larger than the size of the quantum system of atomic dimension (long wavelength approximation). Then, we can invoke in addition the electric-dipole approximation. Given the dipole moment $\boldsymbol{\mu}(\boldsymbol{x})$, the interaction energy between the quantum system and the classical electric field $\boldsymbol{E}(t)$ is given by

$$V(\boldsymbol{x}, t) = -\boldsymbol{\mu}(\boldsymbol{x}) \cdot \boldsymbol{E}(t), \tag{5.1}$$

which, for a perpetually applied monochromatic field of amplitude $\boldsymbol{E}_0$ and angular frequency ω, reduces to

$$V(\boldsymbol{x}, t) = -\boldsymbol{\mu}(\boldsymbol{x}) \cdot \boldsymbol{E}_0 \sin(\omega t + \phi). \tag{5.2}$$

In many circumstances only a finite number of quantum levels strongly interact under the influence of the time-dependent laser field. This means that a truncation to a multi-level quantum system in which only a finite number of quantum states strongly interact is adequate. In particular, the truncation to two relevant levels only, i.e., the so called driven two-level system (TLS), is of enormous practical importance, cf. Sect. 5.4. Setting $\Delta = E_2 - E_1$, this truncation in the energy representation of the ground state $|1\rangle$ and excited state $|2\rangle$ is in terms of the Pauli spin matrices σ_z and σ_x given by

$$H_{\mathrm{TLS}}(t) = -\frac{1}{2}\Delta\sigma_z - \mu E_0 \sin(\omega t + \phi)\sigma_x, \tag{5.3}$$

with $\mu \equiv \langle 2|x|1\rangle$ being the transition dipole moment. Here we have used a scalar approximation of the field $\boldsymbol{E}_0$ in x-direction. The linearly polarized field in (5.3) can, with $2\hbar\lambda \equiv \mu E_0$, be regarded as a superposition of left and right circularly polarized radiation, namely setting $\phi = \pi/2$ we have

$$2\lambda \cos\omega t = \lambda \exp(-\mathrm{i}\omega t) + \lambda \exp(\mathrm{i}\omega t). \tag{5.4}$$

For the absorption process $|1, n\rangle \to |2, n-1\rangle$, the term $\lambda \exp(-\mathrm{i}\omega t)$ supplies the energy $\hbar\omega$ to the system. It corresponds to the rotating-wave (RW) term, while the term $\lambda \exp(\mathrm{i}\omega t)$ is called the anti-rotating-wave term. This anti-RW term removes the energy $\hbar\omega$ from the system, i.e., $|1, n\rangle \to |2, n+1\rangle$, and is thus energy nonconserving. Likewise, the process of emission $|2, n\rangle \to |1, n+1\rangle$ is a RW term, while the second order process $|2, n\rangle \to |1, n-1\rangle$ is again an energy nonconserving anti-RW term.

5.2.2 Spin magnetic resonance

In electron-spin resonance (ESR), nuclear magnetic-spin resonance (NMR) or atomic-beam spectroscopy, a particle of total angular momentum $J = \hbar/2$ is placed in both a static magnetic field B_0 in the z-direction, and a time-dependent oscillating magnetic field $2B_1 \cos(\omega t)$ in x-direction. The magnetic moment of the particle is $\mu = \gamma J$, where γ is the gyromagnetic ratio. Therefore the Hamiltonian H_{SMR} for the particle in the time-dependent magnetic field thus reads

$$H_{\mathrm{SMR}}(t) = -\boldsymbol{\mu} \cdot \boldsymbol{B} = -\frac{1}{2}\hbar\gamma\sigma_z B_0 - \hbar\gamma\sigma_x B_1 \cos(\omega t), \tag{5.5}$$

where $(\sigma_x, \sigma_y, \sigma_z)$ are the Pauli matrices so that the spin is given by $\hbar\boldsymbol{\sigma}/2$. With

$$\Delta = \hbar\gamma B_0 \tag{5.6}$$

and

$$\mu E_0 = 2\hbar\lambda = \hbar\gamma B_1, \tag{5.7}$$

this Hamiltonian coincides with the laser-driven TLS in (5.3).

5.3 Floquet and generalized Floquet theory

5.3.1 Floquet theory

With intense fields interacting with the system, it is well known [11, 12] that the semiclassical theory (treating the field as a classical field) provides results that are equivalent to those obtained from a fully quantized theory whenever fluctuations in the photon number (which, for example, are of importance for spontaneous radiation processes) can safely be neglected. We shall be interested first in the investigation of quantum systems with their Hamiltonian being a periodic function in time,

$$H(t) = H(t+T), \tag{5.8}$$

where T is the period of the perturbation. The symmetry of the Hamiltonian under discrete time translations, $t \to t+T$, enables the use of the Floquet formalism [13]. This formalism is the appropriate vehicle to study strongly driven periodic quantum systems: Not only does it respect the periodicity of the perturbation at all levels of approximation, but its use intrinsically avoids also the occurrence of so-called secular terms, terms that are linear or not periodic in the time variable. The latter characteristically occur in the application of conventional Rayleigh-Schrödinger time-dependent perturbation theory. The Schrödinger equation for the quantum system may be written with the restriction to a one-dimensional system, as

$$\left(H(x,t) - \mathrm{i}\hbar\frac{\partial}{\partial t}\right)\Psi(x,t) = 0. \tag{5.9}$$

With

$$H(x,t) = H_0(x) + V(x,t), \qquad V(x,t) = V(x,t+T), \tag{5.10}$$

the unperturbed Hamiltonian $H_0(x)$ is assumed to possess a complete orthonormal set of eigenfunctions $\{\varphi_n(x)\}$ with corresponding eigenvalues $\{E_n\}$. According to the Floquet theorem, there exist solutions to (5.9) that have the form (so-called Floquet-state solution) [13]

$$\Psi_\alpha(x,t) = \exp(-\mathrm{i}\epsilon_\alpha t/\hbar)\Phi_\alpha(x,t), \tag{5.11}$$

where $\Phi_\alpha(x,t)$ is periodic in time, i.e., it is a Floquet mode obeying

$$\Phi_\alpha(x,t) = \Phi_\alpha(x,t+T). \tag{5.12}$$

Here, ϵ_α is a real parameter, being unique up to multiples of $\hbar\omega$, $\omega = 2\pi/T$. It is termed the Floquet characteristic exponent, or the quasienergy [11, 12]. The term quasienergy reflects the formal analogy with the quasimomentum $\boldsymbol{k}$, characterizing the Bloch eigenstates in a periodic solid. Upon substituting (5.11) into (5.9), one obtains the eigenvalue equation for the quasienergy ϵ_α. With the Hermitian operator

$$\mathcal{H}(x,t) \equiv H(x,t) - \mathrm{i}\hbar\frac{\partial}{\partial t}, \tag{5.13}$$

one finds that

$$\mathcal{H}(x,t)\Phi_\alpha(x,t) = \epsilon_\alpha \Phi_\alpha(x,t). \tag{5.14}$$

We immediately notice that the Floquet modes

$$\Phi_{\alpha'}(x,t) = \Phi_\alpha(x,t)\exp(\mathrm{i}n\omega t) \equiv \Phi_{\alpha n}(x,t) \tag{5.15}$$

with n being an integer number $n = 0, \pm 1, \pm 2, \ldots$ yields the identical solution to that in (5.11), but with the shifted quasienergy

$$\epsilon_\alpha \to \epsilon_{\alpha'} = \epsilon_\alpha + n\hbar\omega \equiv \epsilon_{\alpha n}. \tag{5.16}$$

Hence, the index α corresponds to a whole class of solutions indexed by $\alpha' = (\alpha, n)$, $n = 0, \pm 1, \pm 2, \ldots$. The eigenvalues $\{\epsilon_\alpha\}$ therefore can be mapped into a first Brillouin zone, obeying $-\hbar\omega/2 \leq \epsilon < \hbar\omega/2$. For the Hermitian operator $\mathcal{H}(x,t)$ it is convenient to introduce the composite Hilbert space $\mathcal{R} \otimes \mathcal{T}$ made up of the Hilbert space $\mathcal{R}$ of square integrable functions on configuration space and the space $\mathcal{T}$ of functions which are periodic in t with period $T = 2\pi/\omega$ [14]. For the spatial part the inner product is defined by

$$\langle \varphi_n | \varphi_m \rangle \equiv \int \mathrm{d}x\, \varphi_n^*(x)\varphi_m(x) = \delta_{n,m}, \tag{5.17}$$

while the temporal part is spanned by the orthonormal set of Fourier vectors $\langle t|n\rangle \equiv \exp(\mathrm{i}n\omega t)$, $n = 0, \pm 1, \pm 2, \ldots$, and the inner product in $\mathcal{T}$ reads

$$(m,n) = \frac{1}{T}\int_0^T \mathrm{d}t \exp[\mathrm{i}(n-m)\omega t] = \delta_{n,m}. \tag{5.18}$$

Thus, the eigenvectors of $\mathcal{H}$ obey the orthonormality condition in the composite Hilbert space $\mathcal{R} \otimes \mathcal{T}$,

$$\langle\langle \Phi_{\alpha'}(t) | \Phi_{\beta'}(t) \rangle\rangle \equiv \frac{1}{T}\int_0^T \mathrm{d}t \int_{-\infty}^{\infty} \mathrm{d}x\, \Phi_{\alpha'}^*(x,t)\Phi_{\beta'}(x,t) = \delta_{\alpha',\beta'} = \delta_{\alpha,\beta}\delta_{n,m}, \tag{5.19}$$

and form a complete set in $\mathcal{R} \otimes \mathcal{T}$,

$$\sum_\alpha \sum_n \Phi_{\alpha n}^*(x,t)\Phi_{\alpha n}(y,t') = \delta(x-y)\delta(t-t'). \tag{5.20}$$

Note that in (5.20) we must extend the sum over all Brillouin zones, i.e., over all the representatives n in a class, cf. (5.16). For fixed equal time $t = t'$, the Floquet modes of the first Brillouin zone $\Phi_{\alpha 0}(x,t)$ form a complete set in $\mathcal{R}$,

$$\sum_\alpha \Phi_\alpha^*(x,t)\Phi_\alpha(y,t) = \delta(x-y). \tag{5.21}$$

Clearly, with $t' \neq t + mT = t \pmod T$, the functions $\{\Phi_\alpha^*(x,t), \Phi_\alpha(y,t')\}$ do not form an orthonormal set in $\mathcal{R}$.

5.3.2 General properties of Floquet theory

With a monochromatic perturbation

$$V(x,t) = -Sx\sin(\omega t + \phi) \tag{5.22}$$

the quasienergy ϵ_α is a function of the parameters S and ω, but does not depend on the arbitrary, but fixed phase ϕ. This is so because a shift of the time origin $t_0 = 0 \to t_0 = -\phi/\omega$ will lift a dependence of ϵ_α on ϕ in the quasienergy eigenvalue equation in (5.14). In contrast, the time-dependent Floquet function $\Psi_\alpha(x,t)$ depends, at fixed time, on the phase. The quasienergy eigenvalue equation in (5.14) has the form of the time-independent Schrödinger equation in the composite Hilbert space $\mathcal{R}\otimes\mathcal{T}$. This feature reveals the great advantage of the Floquet formalism: It is now straightforward to use all theorems characteristic for time-independent Schrödinger theory for the periodically driven quantum dynamics, such as the Rayleigh-Ritz variation principle for stationary perturbation theory, the von-Neumann-Wigner degeneracy theorem, or the Hellmann-Feynman theorem, etc.

With $H(t)$ being a time-dependent function, the energy E is no longer conserved. Instead, let us consider the averaged energy in a Floquet state $\Psi_\alpha(x,t)$. This quantity reads

$$\begin{aligned}\bar{H}_\alpha &\equiv \frac{1}{T}\int_0^T \mathrm{d}t\,\langle\Psi_\alpha(x,t)|H(x,t)|\Psi_\alpha(x,t)\rangle \\ &= \epsilon_\alpha + \langle\langle\Phi_\alpha|\mathrm{i}\hbar\frac{\partial}{\partial t}|\Phi_\alpha\rangle\rangle. \end{aligned}\tag{5.23}$$

Invoking a Fourier expansion of the time periodic Floquet function $\Phi_\alpha(x,t) = \sum_k c_k(x)\exp(-\mathrm{i}k\omega t)$, $\sum_k\int\mathrm{d}x|c_k(x)|^2 = 1 = \sum_k\langle c_k|c_k\rangle$, (5.23) can be recast as a sum over k,

$$\bar{H}_\alpha = \epsilon_\alpha + \sum_{k=-\infty}^{\infty}\hbar k\omega\langle c_k|c_k\rangle = \sum_{k=-\infty}^{\infty}(\epsilon_\alpha + \hbar k\omega)\langle c_k|c_k\rangle. \tag{5.24}$$

Hence, $\bar{H}_\alpha$ can be looked upon as the energy accumulated in each harmonic mode of $\Psi_\alpha(x,t) = \exp(-\mathrm{i}\epsilon_\alpha t/\hbar)\Phi_\alpha(x,t)$, and averaged with respect to the weight of each of these harmonics. Moreover, one can apply the Hellmann-Feynman theorem,

$$\frac{\mathrm{d}\epsilon_\alpha(\omega)}{\mathrm{d}\omega} = \langle\langle\Phi(\omega)|\frac{\partial\mathcal{H}(\omega)}{\partial\omega}|\Phi(\omega)\rangle\rangle. \tag{5.25}$$

Setting $\tau = \omega t$ and $\mathcal{H}(x,\tau) = H(x,\tau) - \mathrm{i}\hbar\omega\partial/\partial\tau$, one finds

$$\left(\frac{\partial\mathcal{H}}{\partial\omega}\right)_\tau = -\mathrm{i}\hbar\frac{\partial}{\partial\tau} = -i\hbar\frac{1}{\omega}\frac{\partial}{\partial t} \tag{5.26}$$

and consequently obtains [15]

$$\bar{H}_\alpha = \epsilon_\alpha(S,\omega) - \omega\frac{\partial\epsilon_\alpha(S,\omega)}{\partial\omega}. \tag{5.27}$$

Next we discuss qualitative, general features of quasienergies and Floquet modes with respect to their frequency and field dependence. As mentioned before, if $\epsilon_\alpha = \epsilon_{\alpha 0}$ possesses the Floquet mode $\Phi_{\alpha 0}(x,t)$, the modes

$$\Phi_{\alpha 0} \to \Phi_{\alpha k} = \Phi_{\alpha 0}(x,t)\exp(\mathrm{i}\omega k t), \qquad k = 0, \pm 1, 2, \ldots, \tag{5.28}$$

are also solutions with quasienergies

$$\epsilon_{\alpha k} = \epsilon_{\alpha 0} + \hbar k \omega, \tag{5.29}$$

yielding identical physical states,

$$\begin{aligned}\Psi_{\alpha 0}(x,t) &= \exp(-\mathrm{i}\epsilon_{\alpha 0} t/\hbar)\Phi_{\alpha 0}(x,t) \\ &= \Psi_{\alpha k}(x,t).\end{aligned} \tag{5.30}$$

For an interaction $S \to 0$ that is switched off adiabatically, the Floquet modes and the quasienergies obey

$$\Phi_{\alpha k}(x,t) \stackrel{S\to 0}{\longrightarrow} \Phi^0_{\alpha k}(x,t) = \varphi_\alpha(x)\exp(\mathrm{i}\omega k t) \tag{5.31}$$

and

$$\epsilon_{\alpha k}(S,\omega) \stackrel{S\to 0}{\longrightarrow} \epsilon^0_{\alpha k} = E_\alpha + k\hbar\omega\ , \tag{5.32}$$

with $\{\varphi_\alpha, E_\alpha\}$ denoting the eigenfunctions and eigenvalues of the time-independent part H_0 of the Hamiltonian (5.10). Thus, when $S \to 0$, the quasienergies depend linearly on frequency so that at some frequency values different levels $\epsilon^0_{\alpha k}$ intersect. When $S \neq 0$, the interaction operator mixes these levels, depending on the symmetry properties of the Hamiltonian. Given a symmetry for $H(x,t)$, the Floquet eigenvalues $\epsilon_{\alpha k}$ can be separated into groups: Levels in each group mix with each other, but do not interact with levels of other groups. Let us consider levels $\epsilon^0_{\alpha n}$ and $\epsilon^0_{\beta k}$ of the same group at resonances,

$$E_\alpha + n\hbar\omega_{\mathrm{res}} = E_\beta + k\hbar\omega_{\mathrm{res}} \tag{5.33}$$

with ω_{res} being the frequency of an (unperturbed) resonance. According to the von-Neumann-Wigner theorem [16], these levels of the same group will no longer intersect for finite $S \neq 0$. In other words, these levels develop into avoided crossings (Fig. 5.1a). If the levels obeying (5.33) belong to a different group, for example to different generalized parity states, see below in Sect. 5.5, the quasienergies at finite $S \neq 0$ exhibit exact crossings; cf. Fig. 5.1b.

These considerations, conducted without any approximation, leading to avoided vs. exact crossings, determine many interesting and novel features of driven quantum systems. Some interesting consequences follow immediately from the structure in Fig. 5.1: Starting out from a stationary state $\Psi(x,t) = \varphi_1(x)\exp(-\mathrm{i}E_1 t/\hbar)$ the smooth adiabatic switch-on of the interaction with $\omega < \omega_{\mathrm{res}}$ ($\omega > \omega_{\mathrm{res}}$) will transfer the system into

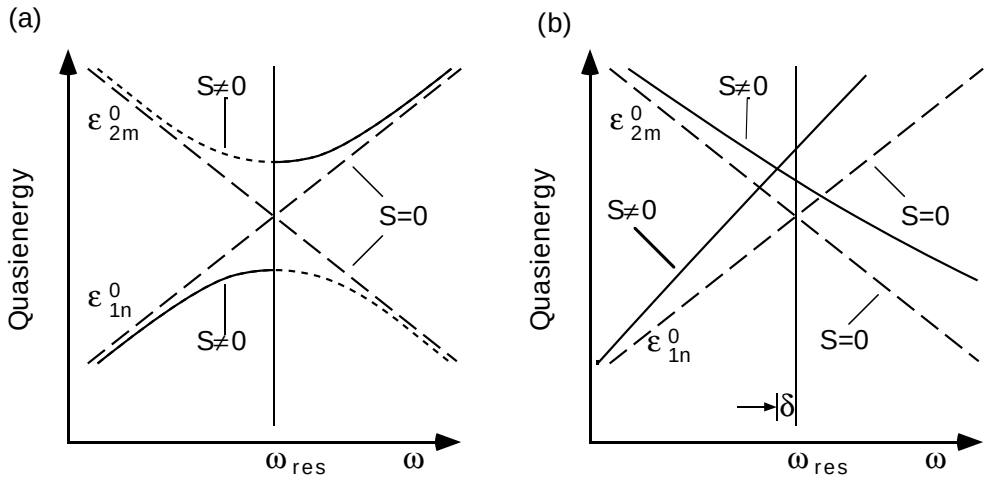

Fig. 5.1: Quasi-energy dependence on frequency ω of a monochromatic electric-dipole perturbation near the unperturbed resonance $\omega_{\rm res}$ between two levels. The dashed lines correspond to quasienergies for $S \to 0$. In panel (a), we depict an avoided crossing for two levels belonging to the same symmetry related group number. Note that with finite S the dotted parts belong to the Floquet mode Φ_{2m}, while the solid parts belong to the state Φ_{1n}. In panel (b), we depict an exact crossing between two members of quasienergies belonging to different symmetry-related groups. With $S \neq 0$, the location of the resonance generally undergoes a shift $\delta = \omega_{\rm res}(S \neq 0) - \omega_{\rm res}(S = 0)$ (so-called Bloch-Siegert shift) [17] that depends on the intensity of S. Only for $S \to 0$ does the resonance frequency coincide with the unperturbed resonance $\omega_{\rm res}$.

a quasienergy state Ψ_{10} [18]. Upon increasing (decreasing) adiabatically the frequency to a value $\omega > \omega_{\rm res}$ ($\omega < \omega_{\rm res}$) and again smoothly switching off the perturbation, the system generally jumps to a different state $\Psi(x,t) = \varphi_2(x)\exp(-{\rm i}E_2 t/\hbar)$. For example, this phenomenon is known in NMR as spin exchange; it relates to a rapid (as compared to relaxation processes) adiabatic crossing of the resonance. Moreover, as seen in Fig. 5.1a, the quasienergy ϵ_{2k} and Floquet mode Φ_{2k} as a function of frequency exhibit jump discontinuities at the frequencies of the unperturbed resonance, i.e., the change of energy between the two parts of the solid lines (or dashed lines, respectively).

5.3.3 Time-evolution operators for Floquet Hamiltonians

The time propagator $K(t,t_0)$, defined by

$$|\Psi(t)\rangle = K(t,t_0)|\Psi(t_0)\rangle, \qquad K(t_0,t_0) = 1, \tag{5.34}$$

assumes special properties when $H(t) = H(t+T)$ is periodic. In particular the propagator over a full period $K(T,0)$ can be used to construct a discrete quantum map, propagating an initial state over long multiples of the fundamental period by observing

$$K(nT,0) = [K(T,0)]^n. \tag{5.35}$$

This important relation follows readily from the periodicity of $H(t)$ and its definition. Namely, we find with $t_0 = 0$ (T denotes time-ordering of operators)

$$K(nT,0) = \mathsf{T}\exp\left[-\frac{\mathrm{i}}{\hbar}\int_0^{nT}\mathrm{d}t\,H(t)\right]$$

$$= \mathsf{T}\exp\left[-\frac{\mathrm{i}}{\hbar}\sum_{k=1}^{n}\int_{(k-1)T}^{kT}\mathrm{d}t\,H(t)\right],$$

which with $H(t) = H(t+T)$ simplifies to

$$K(nT,0) = \mathsf{T}\exp\left[-\frac{\mathrm{i}}{\hbar}\sum_{k=1}^{n}\int_{0}^{T}\mathrm{d}t\,H(t)\right]$$

$$= \mathsf{T}\prod_{k=1}^{n}\exp\left[-\frac{\mathrm{i}}{\hbar}\int_0^{T}\mathrm{d}t\,H(t)\right]. \tag{5.36}$$

Because the terms over a full period are equal, they do commute. Hence the time-ordering operator can be moved in front of a single term, yielding

$$K(nT,0) = \prod_{k=1}^{n}\mathsf{T}\exp\left[-\frac{\mathrm{i}}{\hbar}\int_0^{T}\mathrm{d}t\,H(t)\right]$$

$$= [K(T,0)]^n. \tag{5.37}$$

Likewise, one can show that with $t_0 = 0$ the following relation holds

$$K(t+T,T) = K(t,0), \tag{5.38}$$

which implies that

$$K(t+T,0) = K(t,0)K(T,0). \tag{5.39}$$

Note that $K(t,0)$ does not commute with $K(T,0)$, except at times $t = nT$, so that (5.39) with the right-hand-side product reversed does not hold. A highly important feature of (5.33) — (5.39) is that the knowledge of the propagator over a fundamental period $T = 2\pi/\omega$ provides all the information needed to study the long-time dynamics of periodically driven quantum systems. That is, upon a diagonalization with an unitary transformation S

$$\mathsf{S}^\dagger K(T,0)\mathsf{S} = \exp(-\mathrm{i}\mathsf{D}), \tag{5.40}$$

with D being a diagonal matrix, composed of the eigenphases $\{\epsilon_\alpha T\}$, one obtains

$$K(nT,0) = [K(T,0)]^n = \mathsf{S}\exp(-\mathrm{i}n\mathsf{D})\mathsf{S}^\dagger. \tag{5.41}$$

This relation can be used to propagate any initial state

$$|\Psi(0)\rangle = \sum_\alpha c_\alpha|\Phi_\alpha(0)\rangle, \qquad c_\alpha = \langle\Phi_\alpha(0)|\Psi(0)\rangle. \tag{5.42}$$

in a stroboscopic manner. Such a procedure generates a discrete quantum map. With $\Psi_\alpha(x, t = 0) = \Phi_\alpha(x, t = 0)$, its time evolution follows from (5.11) as

$$\Psi(x,t) = \sum_\alpha c_\alpha \exp(-\mathrm{i}\epsilon_\alpha t/\hbar)\Phi_\alpha(x,t). \tag{5.43}$$

With $\Psi(x,t) = \langle x|K(t,0)|\Psi(0)\rangle$, a spectral representation for the propagator

$$K(x,t;x_0,0) = \langle x|K(t,0)|x_0\rangle, \tag{5.44}$$

follows from (5.44) with $\Psi(x,0) = \delta(x - x_0)$ as

$$K(x,t;x_0,0) = \sum_\alpha \exp(-\mathrm{i}\epsilon_\alpha t/\hbar)\Phi_\alpha(x,t)\Phi^*_\alpha(x_0,0). \tag{5.45}$$

This relation is readily generalized to arbitrary propagation times $t > s$, yielding

$$K(x,t;y,s) = \sum_\alpha \exp(-\mathrm{i}\epsilon_\alpha (t-s)/\hbar)\Phi_\alpha(x,t)\Phi^*_\alpha(y,s). \tag{5.46}$$

Equation (5.46) presents an intriguing result, which generalizes the familiar form of time-independent propagators to time-periodic ones. Note again, however, that the role of the stationary eigenfunction $\varphi_\alpha(x)$ is taken over by the Floquet mode $\Phi_\alpha(x,t)$, being orthonormal only at equal times $t = s$.

5.3.4 Generalized Floquet theory

In the previous subsections we restricted ourselves to pure harmonic interactions. In many physical applications, e.g. see in [8], however, the time-dependent perturbation has an arbitrary, for example, pulse-like form that acts over a limited time regime only. Clearly, in these cases the Floquet theorem cannot readily be applied. This feature forces one to look for a generalization of the quasienergy concept. Before we start doing so, we note that the Floquet eigenvalues $\epsilon_{\alpha n}$ in (5.16) can also be obtained as the ordinary Schrödinger eigenvalues within a two-dimensional formulation of the time-periodic Hamiltonian in (5.10). Setting $\omega t = \theta$, (5.10) is recast as

$$H(t) = H_0(x,p) + V(x,\theta(t)). \tag{5.47}$$

With $\dot\theta = \omega$, one constructs the enlarged Hamiltonian $\widetilde{H}(x,p;\theta,p_\theta) = H_0(x,p) + V(x,\theta) + \omega p_\theta$, where p_θ is the canonically conjugate momentum, obeying

$$\dot\theta = \frac{\partial \widetilde{H}}{\partial p_\theta} = \omega. \tag{5.48}$$

The quantum mechanics of $\widetilde{H}$ acts on the Hilbert space of square-integrable functions on the extended space of the x-variable and the square-integrable periodic functions on the compact space of the unit circle $\theta = \theta_0 + \omega t$ (periodic boundary conditions for θ). With $V(x,t)$ given by (5.22), the Floquet modes $\Phi_{\alpha k}(x,\theta)$ and the quasienergies $\epsilon_{\alpha k}$

are the eigenfunctions and eigenvalues of the two-dimensional stationary Schrödinger equation, i.e., with $[\theta, p_\theta] = \mathrm{i}\hbar$,

$$\left\{ \frac{-\hbar^2}{2m}\frac{\partial^2}{\partial x^2} + V_0(x) - Sx\sin(\theta+\phi) - \mathrm{i}\hbar\omega\frac{\partial}{\partial\theta} \right\} \Phi_{\alpha k}(x,\theta) = \epsilon_{\alpha k}\Phi_{\alpha k}(x,\theta). \tag{5.49}$$

This procedure opens a door to treat more general, polychromatic perturbations composed of generally incommensurate frequencies. For example, a quasiperiodic perturbation with two incommensurate frequencies ω_1 and ω_2,

$$V(x,t) = -xS\sin(\omega_1 t) - xF\sin(\omega_2 t), \tag{5.50}$$

can be enlarged into a six-dimensional phase space $(x, p_x; \theta_1, p_{\theta_1}; \theta_2, p_{\theta_2})$, with $\{\theta_1 = \omega_1 t; \theta_2 = \omega_2 t\}$ defined on a torus. The quantization of the corresponding momentum terms yield a stationary Schrödinger equation in the three variables (x, θ_1, θ_2) with a corresponding Hamiltonian operator $\widetilde{H}$ given by

$$\widetilde{H} = H(x,\theta_1,\theta_2) - \mathrm{i}\hbar\omega_1\frac{\partial}{\partial\theta_1} - \mathrm{i}\hbar\omega_2\frac{\partial}{\partial\theta_2} \tag{5.51}$$

with eigenvalues $\{\epsilon_{\alpha,k_1,k_2}\}$ and generalized stationary wavefunctions given by the generalized Floquet modes $\Phi_{\alpha,k_1,k_2}(x,\theta_1,\theta_2) = \Phi_{\alpha,k_1,k_2}(x;\theta_1+2\pi;\theta_2+2\pi)$. We note that with quasiperiodic driving the spectrum may become rather complex, consisting generally of spectral parts that are pure point, absolutely continuous or even singular continuous.

A general perturbation, such as a time-dependent laser-pulse interaction consists (via Fourier-integral representation) of an infinite number of frequencies, so that the above embedding ceases to be of practical use. The general time-dependent Schrödinger equation

$$\mathrm{i}\hbar\frac{\partial}{\partial t}\Psi(x,t) = H(x,t)\Psi(x,t), \tag{5.52}$$

with the initial state given by

$$\Psi(x,t_0) = \Psi_0(x), \tag{5.53}$$

can be solved by numerical means, by a great variety of methods [19–21]. All these methods must involve efficient numerical algorithms to calculate the time-ordered propagation operator $K(t,s)$. Generalizing the idea of Shirley [11] and Sambe [14] for time-periodic Hamiltonians, it is possible to introduce a Hilbert space for general time-dependent Hamiltonians in which the Schrödinger equation becomes time independent. Following the reasoning by Howland [22], we introduce the reader to the so called (t,t')-formalism [23].

5.3.5 The (t,t')-formalism

The time-dependent solution

$$\Psi(x,t) = K(t,t_0)\Psi(x,t_0) \tag{5.54}$$

for the explicitly time-dependent Schrödinger equation in (5.52) can be obtained as

$$\Psi(x,t) = \Psi(x,t',t)|_{t'=t}, \tag{5.55}$$

where

$$\Psi(x,t',t) = \exp\left(-\frac{\mathrm{i}}{\hbar}\mathcal{H}(x,t')(t-t_0)\right)\Psi(x,t',t_0). \tag{5.56}$$

$\mathcal{H}(x,t')$ is the generalized Floquet operator

$$\mathcal{H}(x,t') = H(x,t') - \mathrm{i}\hbar\frac{\partial}{\partial t'}. \tag{5.57}$$

The time t' acts as a time coordinate in the generalized Hilbert space of square-integrable functions of x and t', where a box normalization of length T is used for t' $(0 < t' < T)$. For two functions $\phi_\alpha(x,t), \phi_\beta(x,t)$ the inner, or scalar product reads

$$\langle\langle\phi_\alpha|\phi_\beta\rangle\rangle = \frac{1}{T}\int_0^T \mathrm{d}t' \int_{-\infty}^{\infty} \mathrm{d}x\ \phi_\alpha^*(x,t')\phi_\beta(x,t'). \tag{5.58}$$

The proof for (5.55) can readily be given as follows [23]: Note that from (5.56)

$$\begin{aligned}\mathrm{i}\hbar\frac{\partial}{\partial t}\Psi(x,t',t) &= \mathcal{H}(x,t')\exp[-\mathrm{i}\mathcal{H}(x,t')(t-t_0)/\hbar]\Psi(x,t',t_0)\\ &= -\mathrm{i}\hbar\frac{\partial}{\partial t'}\Psi(x,t',t) + H(x,t')\Psi(x,t',t).\end{aligned} \tag{5.59}$$

Hence,

$$\mathrm{i}\hbar\left(\frac{\partial}{\partial t} + \frac{\partial}{\partial t'}\right)\Psi(x,t',t) = H(x,t')\Psi(x,t',t). \tag{5.60}$$

Since we are interested in t' only on the contour $t' = t$, where $\partial t'/\partial t = 1$, one therefore finds that

$$\left.\frac{\partial\Psi(x,t',t)}{\partial t'}\right|_{t'=t} + \left.\frac{\partial\Psi(x,t',t)}{\partial t}\right|_{t'=t} = \frac{\partial\Psi(x,t)}{\partial t}, \tag{5.61}$$

which with (5.60) for $t = t'$ consequently proves the assertion in (5.55).

Note that a long time propagation now requires the use of a large box, i.e. the time period T must be chosen sufficiently large. If we are not interested in the very-long-time propagation, the perturbation of finite duration can be embedded into a box of finite length T, and periodically continued. This so constructed perturbation now implies a time-periodic Hamiltonian, so that we require time periodic boundary conditions

$$\Psi(x,t',t) = \Psi(x,t'+T,t), \tag{5.62}$$

with $0 \le t' \le T$, and the physical solution is obtained when

$$t' = t \bmod T. \tag{5.63}$$

Stationary solutions of (5.59) reduce to the Floquet states, as found before, namely

$$\Psi_\alpha(x,t',t) = \exp(-\mathrm{i}\epsilon_\alpha t/\hbar)\Phi_\alpha(x,t'), \tag{5.64}$$

with $\Phi_\alpha(x,t') = \Phi_\alpha(x,t'+T)$, and $t' = t \bmod T$. We remark that although $\Psi(x,t',t)$, $\Psi_\alpha(x,t',t)$ are periodic in t', the solution $\Psi(x,t) = \Psi(x,t'=t,t)$ is generally not time periodic.

The (t,t')-method hence avoids the need to introduce the generally nasty time-ordering procedure. Expressed differently, the step-by-step integration that characterizes the time-dependent approaches is not necessary when formulated in the above generalized Hilbert space where $\mathcal{H}(x,t')$ effectively becomes time-independent, with t' acting as coordinate. Formally, the result in (5.59) can be looked upon as quantizing the new Hamiltonian $\widehat{H}$, defined by

$$\widehat{H}(x,p;E,t') = H(x,p,t') - E, \tag{5.65}$$

using for the operator $E \to \widehat{E}$ the canonical quantization rule $\widehat{E} = \mathrm{i}\hbar\partial/\partial t$; with $[\widehat{E},\widehat{t}] = \mathrm{i}\hbar$ and $\widehat{t}\phi(t) = t\phi(t)$. This formulation of the time-dependent problem in (5.52) within the auxiliary t' coordinate is particularly useful for evaluating the state-to-state transition probabilities in pulse-sequence-driven quantum systems [8, 23].

5.4 Exactly solvable driven quantum systems

In contrast to time-independent quantum theory, exactly solvable quantum systems with time-dependent potentials are extremely rare. One such class of exactly solvable systems are (multidimensional) systems with at most quadratic interactions between momentum and coordinate operators, e. g. the parametrically driven harminic oscillator [24, 25], including generalizations that account for quantum dissipation via bilinear coupling to a harmonic bath [26], see also chapter 4.

Further, we note that a Hamiltonian part that depends solely on time t can always be absorbed into an overall time-dependent phase of the wavefunction. This is so, because such an interaction cannot affect the spatial dependence of the wavefunction.

5.4.1 Driven quantum oscillators

The Schrödinger equation of a harmonic oscillator with an arbitrary time-dependent dipole interaction reads

$$\mathrm{i}\hbar\dot{\Psi}(x,t) = \left\{-\frac{\hbar^2}{2m}\frac{\partial^2}{\partial x^2} + \frac{1}{2}m\omega_0^2 x^2 - xS(t)\right\}\Psi(x,t). \tag{5.66}$$

Following the reasoning by Husimi [24], this system can be solved explicitly. First we introduce the shifted coordinate

$$x \to y = x - \zeta(t), \tag{5.67}$$

yielding

$$\mathrm{i}\hbar\dot{\Psi}(y,t) = \left\{\mathrm{i}\hbar\dot{\zeta}\frac{\partial}{\partial y} - \frac{\hbar^2}{2m}\frac{\partial^2}{\partial y^2} + \frac{1}{2}m\omega_0^2(y+\zeta)^2 - (y+\zeta)S(t)\right\}\Psi(y,t). \tag{5.68}$$

Performing the unitary transformation

$$\Psi(y,t) = \exp\{-\mathrm{i}m\dot{\zeta}y/\hbar\}\phi(y,t), \tag{5.69}$$

with $\zeta(t)$ obeying the classical equation of motion,

$$m\ddot{\zeta} + m\omega_0^2\zeta = S(t), \tag{5.70}$$

the term linear in y vanishes to yield

$$\mathrm{i}\hbar\dot{\phi}(y,t) = \left\{-\frac{\hbar^2}{2m}\frac{\partial^2}{\partial y^2} + \frac{1}{2}m\omega_0^2y^2 + L(\zeta,\dot{\zeta},t)\right\}\phi(y,t). \tag{5.71}$$

Here, $L(\zeta,\dot{\zeta},t)$ is the classical Lagrangian of a driven oscillator,

$$L = \frac{1}{2}m\dot{\zeta}^2 - \frac{1}{2}m\omega_0^2\zeta^2 + \zeta S(t). \tag{5.72}$$

Another unitary transformation

$$\phi(y,t) = \exp\left\{-\mathrm{i}\int_0^t \mathrm{d}t' L(\zeta,\dot{\zeta},t')\right\}\chi(y,t) \tag{5.73}$$

reduces the starting equation to the well-known Schrödinger equation of a stationary harmonic oscillator,

$$\mathrm{i}\hbar\dot{\chi}(y,t) = \left\{-\frac{\hbar^2}{2m}\frac{\partial^2}{\partial y^2} + \frac{1}{2}m\omega_0^2y^2\right\}\chi(y,t). \tag{5.74}$$

In terms of the eigenvalues $E_n = \hbar\omega_0(n+1/2)$, and the well-known harmonic eigenfunctions φ_n, being proportional to the Hermite functions, the solutions of (5.66) are of the form

$$\Psi_n(x,t) = \varphi_n\left(x-\zeta(t)\right)\exp\left\{\frac{\mathrm{i}}{\hbar}\left[m\dot{\zeta}(t)(x-\zeta(t)) - E_nt + \int_0^t \mathrm{d}t'\,L\right]\right\}. \tag{5.75}$$

The set $\{\varphi_n(x)\}$ forms a complete set in $\mathcal{R}$; thus any general solution $\Psi(x,t)$ can be expanded in terms of the solutions in (5.75). Next we consider the restriction to a periodic monochromatic drive

$$S(t) = S\sin(\omega t+\phi), \qquad \omega \neq \omega_0. \tag{5.76}$$

A periodic solution ζ_ϕ of (5.70) reads

$$m\zeta_\phi(t) = S\sin(\omega t+\phi)/(\omega_0^2-\omega^2). \tag{5.77}$$

The quasienergies $\{\epsilon_\alpha\}$ and the Floquet modes $\Phi_\alpha(x,t)$ can be deduced from (5.75) if we add — and subtract — the term that is linearly increasing in time,

$$\frac{t}{T}\int_0^T \mathrm{d}t' L(\zeta,\dot{\zeta},t') = \frac{S^2}{4m(\omega_0^2-\omega^2)}t. \tag{5.78}$$

Hence, the quasienergies can readily be read off, to give

$$\epsilon_\alpha = \hbar\omega_0(\alpha+1/2) - \frac{S^2}{4m(\omega_0^2-\omega^2)}\,, \qquad \alpha = 0,1,2,\ldots, \tag{5.79}$$

with corresponding time-periodic Floquet modes

$$\begin{aligned}\Phi_\alpha(x,t) &= \varphi_\alpha\left(x-\zeta_\phi(t)\right)\\ &\quad\times\exp\left\{\frac{i}{\hbar}\left[m\dot{\zeta}_\phi(t)(x-\zeta_\phi(t)) + \left(\int_0^t \mathrm{d}t' L - \frac{t}{T}\int_0^T \mathrm{d}t' L\right)\right]\right\}.\end{aligned} \tag{5.80}$$

Note that at resonance, $\omega=\omega_0$, the quasienergies in (5.79) are no longer correct. Instead, the spectrum assumes an absolutely continuous form [25]. Likewise, the harmonically driven parabolic barrier (i.e. the inverted harmonic potential $\omega_0^2x^2/2 \to -\omega_0^2x^2/2$), can be treated analogously, with the eigenfunctions φ_n becoming parabolic cylinder functions. The resulting quasienergies are continuous, reading

$$\epsilon_\alpha = \alpha + \frac{S^2}{4m(\omega_0^2+\omega^2)} \tag{5.81}$$

with $\alpha\in(-\infty,\infty)$. Due to the reflection symmetry in (5.66), (5.76), i.e., $x\to -x, t\to t+\pi/\omega$, this continuum $\{\epsilon_\alpha\}$ is doubly degenerate.

5.4.2 Periodically driven two-level systems

The problem of a time-dependently driven two level dynamics is of enormous practical importance in nuclear magnetic resonance, quantum optics, or in low temperature glass systems, to name only a few. The driven two-level system has a long history, and reviews are available [27]. A pioneering piece of work must be attributed to Rabi [28] who considered the two-level system in a circularly polarized magnetic field — a problem that he could solve exactly, see below. He thereby elucidated how to measure simultaneously both the sign as well as the magnitude of magnetic moments. However, as Bloch and Siegert experienced soon after [17], this problem is no longer exactly solvable in analytical closed form when the field is linearly polarized, rather than circularly. We set for the wavefunction

$$\Psi(t) = c_1(t)\exp(\mathrm{i}\Delta t/2\hbar)\begin{pmatrix}1\\0\end{pmatrix} + c_2(t)\exp(-\mathrm{i}\Delta t/2\hbar)\begin{pmatrix}0\\1\end{pmatrix} \tag{5.82}$$

where $|c_1(t)|^2 + |c_2(t)|^2 = 1$. With $2\hbar\lambda \equiv -\mu E_0$ and $\varphi = \pi/2$, yielding a pure $\cos(\omega t)$ perturbation, the Schrödinger equation has the form

$$\mathrm{i}\hbar\frac{\mathrm{d}}{\mathrm{d}t}\begin{pmatrix} c_1(t)\exp(\mathrm{i}\Delta t/2\hbar) \\ c_2(t)\exp(-\mathrm{i}\Delta t/2\hbar) \end{pmatrix}$$

$$= \begin{pmatrix} -\Delta/2 & -2\hbar\lambda\cos\omega t \\ -2\hbar\lambda\cos\omega t & \Delta/2 \end{pmatrix}\begin{pmatrix} c_1(t)\exp(\mathrm{i}\Delta t/2\hbar) \\ c_2(t)\exp(-\mathrm{i}\Delta t/2\hbar) \end{pmatrix}. \qquad (5.83)$$

With $\hbar\omega_0 \equiv \Delta$, (5.83) provides two coupled first-order equations for the amplitudes,

$$\frac{\mathrm{d}c_1}{\mathrm{d}t} = \mathrm{i}\lambda\Big(\exp[\mathrm{i}(\omega-\omega_0)t] + \exp[-\mathrm{i}(\omega+\omega_0)t]\Big)c_2,$$

$$\frac{\mathrm{d}c_2}{\mathrm{d}t} = \mathrm{i}\lambda\Big(\exp[-\mathrm{i}(\omega-\omega_0)t] + \exp\mathrm{i}(\omega+\omega_0)t]\Big)c_1. \qquad (5.84)$$

With an additional differentiation with respect to time, and substituting $\dot{c}_2$ from the second equation, we readily find that $c_1(t)$ obeys a linear second order ordinary differential equation with time periodic ($T = 2\pi/\omega$) coefficients (Hill equation). Clearly, such equations are generally not solvable in analytical closed form. Hence, although the problem is simple, the job of finding an analytical solution presents a hard task! To make progress, one usually invokes, at this stage, the so-called rotating-wave approximation (RWA), assuming that ω is close to ω_0 (near resonance), and λ not very large. Then the anti-rotating-wave term $\exp(\mathrm{i}(\omega+\omega_0)t)$ is rapidly varying, as compared to the slowly varying rotating-wave term $\exp(-\mathrm{i}(\omega-\omega_0)t)$. Therefore it cannot transfer much population from state $|1\rangle$ to state $|2\rangle$. Neglecting this anti-rotating contribution, one has in terms of the detuning parameter $\delta \equiv \omega - \omega_0$,

$$\frac{\mathrm{d}c_1}{\mathrm{d}t} = \mathrm{i}\lambda\exp(\mathrm{i}\delta t)c_2, \qquad \frac{\mathrm{d}c_2}{\mathrm{d}t} = \mathrm{i}\lambda\exp(-\mathrm{i}\delta t)c_1. \qquad (5.85)$$

From (5.83) one finds for $c_1(t)$ a linear second-order differential equation with constant coefficients — which can be solved readily for arbitrary initial conditions. For example, setting $c_1(0) = 1$, $c_2(0) = 0$, one obtains

$$c_1(t) = \exp(\mathrm{i}\delta t)\left[\cos\left(\frac{1}{2}\Omega t\right) - \mathrm{i}\frac{\delta}{\Omega}\sin\left(\frac{1}{2}\Omega t\right)\right],$$

$$c_2(t) = \exp(-\mathrm{i}\delta t)\frac{2\mathrm{i}\lambda}{\Omega}\sin\left(\frac{1}{2}\Omega t\right), \qquad (5.86)$$

where Ω denotes the celebrated Rabi frequency

$$\Omega = \left(\delta^2 + 4\lambda^2\right)^{1/2}. \qquad (5.87)$$

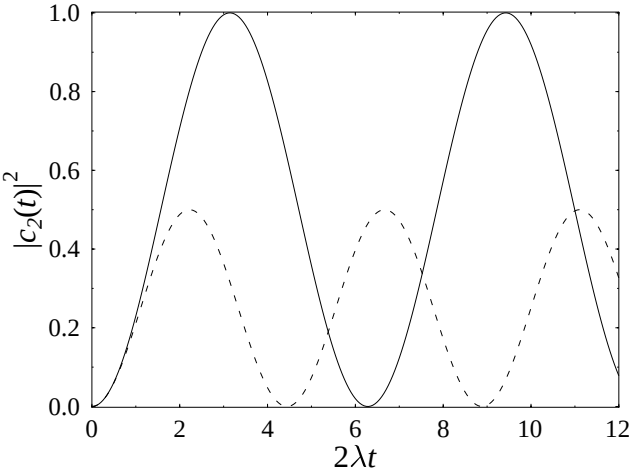

Fig. 5.2: The population probability of the upper state $|c_2(t)|^2$ as a function of time t at resonance $\delta = 0$ (solid line), versus the non-resonant excitation dynamics (dashed line) at $\delta = 2\lambda \neq 0$.

The populations as a function of time are then given by

$$|c_1(t)|^2 = \left(\frac{\delta}{\Omega}\right)^2 + \left(\frac{2\lambda}{\Omega}\right)^2 \cos^2\left(\frac{1}{2}\Omega t\right), \tag{5.88}$$

$$|c_2(t)|^2 = \left(\frac{2\lambda}{\Omega}\right)^2 \sin^2\left(\frac{1}{2}\Omega t\right). \tag{5.89}$$

Note that at short times t, the excitation in the upper state is independent of the detuning, $|c_2(t)|^2 \longrightarrow \lambda^2 t^2$ for $\Omega t \ll 1$. This behavior is in accordance with perturbation theory, valid at small times. Moreover, the population at resonance $\omega = \omega_0$ completely cycles the population between the two states, while with $\delta \neq 0$, the lower state is never completely depopulated, see Fig. 5.2.

Up to now, we have discussed approximate RWA solutions. At this point we remark that the unitary transformation

$$H_{\rm T} = U^{-1} H_{\rm TLS} U, \qquad U = \exp(\mathrm{i}\pi\sigma_y/4) \tag{5.90}$$

transforms the Hamiltonian in (5.3) into the form

$$H_{\rm T} = -\frac{1}{2}\Delta\sigma_x + 2\hbar\lambda\sin(\omega t + \phi)\sigma_z. \tag{5.91}$$

This is the appropriate representation for tunneling problems, $H_{\rm T}$. Appropriate basis states are the "localized" (right/left) wavefunctions $|\pm\rangle = (|1\rangle \pm |2\rangle)/\sqrt{2}$, which are eigenstates of σ_z with the eigenvalues ± 1. The form given for $H_{\rm TLS}$ is convenient

for the description of optical properties such as the dipole moment. We have for the expectation

$$\mu(t) = \mathrm{tr}\{\varrho_{\mathrm{TLS}}\sigma_x\} = \mathrm{tr}\{\varrho_{\mathrm{T}}\sigma_z\}, \tag{5.92}$$

where $\varrho_{\ldots}$ is the density matrix in the corresponding representation. Note that a static asymmetry energy can be included if the field assumes a static component, i.e. $\lambda\sin(\omega t+\phi) \to \lambda\sin(\omega t+\phi)+\lambda_0$.

Explicit results for the time-periodic Schrödinger equation require numerical methods, cf. Sect. 5.5, one must solve for the quasienergies $\epsilon_{\alpha n}$ and the Floquet modes $\Psi_{\alpha n}(x,t)$. Without proof we state here some results that are very important in discussing driven tunneling in the deep quantum regime. For example, Shirley [11] already showed that in the high-frequency regime $\Delta \ll \max[\omega, (\lambda\omega)^{1/2}]$ the quasienergies obey the difference

$$\epsilon_{2,-1} - \epsilon_{1,1} = \hbar\omega_0 J_0(4\lambda/\omega), \tag{5.93}$$

where J_0 denotes the zeroth order Bessel function of the first kind. The sum of the two quasienergies obeys the rigorous relation [11]

$$\epsilon_{2n} + \epsilon_{1k} = E_1 + E_2 = 0 \pmod{\hbar\omega}. \tag{5.94}$$

For weak fields, one can evaluate the quasienergies by use of the stationary perturbation theory in the composite Hilbert space $\mathcal{R}\otimes\mathcal{T}$. In this way one finds:

(i) Exact crossings at the parity forbidden transitions where $\omega_0 = 2n\omega, n = 1, 2, \ldots$, so that

$$\epsilon_{2,1} = 0 \pmod{\hbar\omega}. \tag{5.95}$$

(ii) At resonance $\omega = \omega_0$:

$$\epsilon_{2,1} = \pm\frac{1}{2}\hbar\omega_0\left(1 + \frac{2\lambda}{\omega_0}\sqrt{1-\lambda^2/4\omega_0^2}\right) \pmod{\hbar\omega}. \tag{5.96}$$

(iii) Near resonance, one finds from the RWA approximation readily the result

$$\epsilon_{2,1} = \pm\frac{1}{2}\hbar\omega\left(1 + \frac{\Omega}{\omega}\right) \pmod{\hbar\omega}, \tag{5.97}$$

where Ω denotes the Rabi frequency in (5.87). Correcting this result for counter-rotating terms, an improved result, up to order $\mathrm{O}(\lambda^6)$, reads [27]

$$\epsilon_{2,1} = \pm\frac{1}{2}\hbar\omega\left(1 + \frac{\bar{\Omega}}{\omega}\right) \pmod{\hbar\omega}, \tag{5.98}$$

with the effective Rabi frequency $\bar{\Omega}$

$$\bar{\Omega}^2 = \delta^2 + \frac{8\omega_0\lambda^2}{(\omega+\omega_0)} - \frac{8\omega_0\lambda^4}{(\omega+\omega_0)^3}. \tag{5.99}$$

Notice that the maximum of the time-averaged transition probability in (5.89) occurs within RWA precisely at $\omega = \omega_0$. This result no longer holds with (5.99) where the maximum with $\Omega \to \bar{\Omega}$ in (5.88) undergoes a shift, termed the Bloch-Siegert shift $\omega_{\rm res} \neq \omega_0$ [17, 27]. From $(\partial\bar{\Omega}^2/\partial\omega_0)_\lambda = 0$ this shift is evaluated as [17, 27].

$$\omega_{\rm res} = \omega_0 + \frac{\lambda^2}{\omega_0} + \frac{\lambda^4}{4\omega_0^3}. \tag{5.100}$$

This Bloch-Siegert shift presents a characteristic measure of the deviation beyond the RWA-approximation, as a result of the nonzero anti-rotating terms in (5.84).

Let us next explicitly consider the case pioneered by Rabi [28], a TLS driven in a spatially homogeneous, circularly polarized external radiation field. This leads to the Hamiltonian

$$\begin{aligned} H(t) &= -\frac{1}{2}\hbar\omega_0\sigma_z - 2\hbar\lambda\,(\sigma_x\cos\omega t - \sigma_y\sin\omega t) \\ &= -\frac{1}{2}\hbar\begin{pmatrix} -\omega_0 & 4\lambda\exp(\mathrm{i}\omega t) \\ 4\lambda\exp(-\mathrm{i}\omega t) & \omega_0 \end{pmatrix}. \end{aligned} \tag{5.101}$$

Absorbing the phase $\exp(\pm\mathrm{i}\omega_0 t)$ into the time-dependence of the coefficients, i.e., setting $a_{1,2}(t) = c_{1,2}(t)\exp(\pm\mathrm{i}\omega_0 t)$, we rotate the states around the z-axis by the amount ωt. With $S_z = \hbar\sigma_z/2$, one has

$$\begin{pmatrix} b_1(t) \\ b_2(t) \end{pmatrix} = \exp\left(-\frac{\mathrm{i}}{\hbar}S_z\omega t\right)\begin{pmatrix} a_1(t) \\ a_2(t) \end{pmatrix} = \begin{pmatrix} a_1(t)\exp(-\mathrm{i}\omega t/2) \\ a_2(t)\exp(+\mathrm{i}\omega t/2) \end{pmatrix}. \tag{5.102}$$

Upon a substitution of (5.101) and (5.102) into the time-dependent Schrödinger equation, and collecting all the terms, results in a time-independent Schrödinger equation for the states $(b_1(t), b_2(t))$, which reads

$$\begin{aligned} -\mathrm{i}\dot{b}_1 &= -\frac{1}{2}(\omega - \omega_0)b_1 + \lambda b_2, \\ -\mathrm{i}\dot{b}_2 &= \lambda b_1 + \frac{1}{2}(\omega - \omega_0)b_2. \end{aligned} \tag{5.103}$$

Hence, one obtains a harmonic oscillator equation for $b_1(t)$ (and similarly for $b_2(t)$),

$$\ddot{b}_1 + \left(\lambda^2 + \frac{\delta^2}{4}\right)b_1 = 0. \tag{5.104}$$

It describes an oscillation with frequency $\frac{1}{2}\Omega = \sqrt{\lambda^2 + \delta^2/4}$, where Ω coincides precisely with the previously found Rabi frequency in (5.87). With $c_1(0) = a_1(0) = b_1(0) = 1$, and $c_2(0) = a_2(0) = b_2(0) = 0$ the populations are given by the corresponding

relations in (5.88), which in this case are exact. In particular, the transition probability $W_{1\to 2}(t) = |\langle 2|\Psi(t)\rangle|^2 = |a_2(t)|^2 = |b_2(t)|^2 = |c_2(t)|^2$ obeys

$$W_{1\to 2}(t) = \frac{4\lambda^2}{\Omega^2}\sin^2\left(\frac{1}{2}\Omega t\right). \tag{5.105}$$

At resonance, $\delta = 0$, $\omega = \omega_0$, it assumes with $\Omega^2 = 4\lambda^2$ its maximal value. We also note that the quasienergies are given by the — in this case exact — result in (5.96).

5.4.3 Quantum systems driven by circularly polarized fields

The fact that the time evolution of a TLS in a circularly polarized field can be factorized in terms of a time-independent Hamiltonian in (5.103) is surprising. We note that this factorization involves a rotation around the z-axis,

$$|a(t)\rangle \quad \longrightarrow \quad |b(t)\rangle = \exp(-\mathrm{i}S_z\omega t/\hbar)|a(t)\rangle. \tag{5.106}$$

This feature can be generalized to any higher-dimensional system, such as a magnetic system or a general quantum system that can be brought into the structure which, in a representation where J_z is diagonal, is of the form

$$H(t) = H_0(J^2) + H_1(J_z) - 4\lambda[J_x\cos\omega t - J_y\sin\omega t]. \tag{5.107}$$

Here, $H_0(J^2)$ contains all interactions that are rotationally invariant (Coulomb interactions, spin-spin and spin-orbit interactions). Setting $R(t) \equiv \exp(-\mathrm{i}J_z\omega t/\hbar)$ and upon observing that

$$\begin{aligned} R(t)J_xR(t)^{-1} &= J_x\cos\omega t + J_y\sin\omega t, \\ R(t)J_yR(t)^{-1} &= -J_x\sin\omega t + J_y\cos\omega t, \\ R(t)J_zR(t)^{-1} &= J_z, \end{aligned} \tag{5.108}$$

one finds upon substituting (5.108) into (5.107)

$$\widetilde{H}(t) \equiv R(t)H(t)R^{-1}(t) = H_0(J^2) + H_1(J_z) - 4\lambda J_x. \tag{5.109}$$

Hence, the transformed Hamiltonian becomes independent of time. With the propagator obeying

$$\begin{aligned} \frac{\partial}{\partial t}K(t,t_0) &= -\frac{\mathrm{i}}{\hbar}H(t)K(t,t_0) \\ &= -\frac{\mathrm{i}}{\hbar}R^{-1}(t)\widetilde{H}R(t)K(t,t_0), \end{aligned}$$

we find from

$$\frac{\partial}{\partial t}[R(t)K(t,t_0)R^{-1}(t_0)] = -\frac{\mathrm{i}}{\hbar}\widehat{H}[R(t)K(t,t_0)R^{-1}(t_0)] \tag{5.110}$$

where

$$\begin{aligned}\widehat{H} &= \widetilde{H} + \omega J_z \\ &= H_0 + H_1(J_z) - 4\lambda J_x + \omega J_z,\end{aligned} \tag{5.111}$$

that the propagator factorizes into the form

$$K(t,t_0) = \exp\left(\frac{\mathrm{i}}{\hbar} J_z \omega t\right) \exp\left(-\frac{\mathrm{i}}{\hbar}\widehat{H}(t-t_0)\right) \exp\left(-\frac{\mathrm{i}}{\hbar} J_z \omega t_0\right). \tag{5.112}$$

Because $\exp(\mathrm{i}J_z\omega t/\hbar)$ at times $t = 2\pi/\omega$ equals 1 for integer values of the angular momentum and -1, for half-integer values, respectively, the propagator in (5.112) can be recast into the Floquet form in (5.39),

$$K(t+nT,0) = K(t,0)[K(T,0)]^n. \tag{5.113}$$

With $J_z = \pm 1, \pm 2, \ldots$, the Floquet form, cf. (5.38), is achieved already with (5.112). For half-integer spin the corresponding Floquet form is obtained by setting for the propagator

$$\begin{aligned}K(t,t_0) = \exp\left(\frac{\mathrm{i}}{\hbar}\left(J_z + \frac{\hbar}{2}\right)\omega t\right) \exp\left(-\frac{\mathrm{i}}{\hbar}\left(\widehat{H} + \frac{\hbar}{2}\omega\right)(t-t_0)\right) \\ \times \exp\left(-\frac{\mathrm{i}}{\hbar}\left(J_z + \frac{\hbar}{2}\right)\omega t_0\right),\end{aligned} \tag{5.114}$$

since the first and third contribution are now periodic with period T. Given the eigenvalues $\{\widehat{\epsilon}_\alpha\}$ of $\widehat{H}$, the exact quasienergies are given by the relation

$$\epsilon_\alpha = (\widehat{\epsilon}_\alpha + \hbar\omega/2) \bmod \hbar\omega. \tag{5.115}$$

The general results derived here carry a great potential for applications involving time-dependent tunneling of spin in magnetic systems with anisotropy, and strongly driven molecular and quantum optical systems as well.

In summary, we demonstrated that a periodically driven TLS — or a general quantum system of the form in (5.107) — can be solved analytically only when driven by a circularly polarized ac-source. This is the case for the Rabi solution. The situation changes when we instead consider a infinite number of states or a periodic lattice with period L, such as a tight-binding Hamiltonian. Then, a linearly polarized dipole interaction $-[S_0 + S\cos(\omega t)]L\sum_n |n\rangle n\langle n|$ yields the exact quasienergy or Floquet states if $S_0 L = n\hbar\omega$, (where $n = 0$ if $S_0 = 0$); i.e. if the energy of n photons precisely matches the energy difference between adjacent rungs of the corresponding Wannier-Stark ladder [29, 30]. Also, we mention here that an analytical solution can be constructed when the above dipole interaction acts in a quantum well that is sandwiched between two infinitely high walls [31].

5.5 Numerical approaches to periodically driven quantum systems

Except for the special cases discussed in Sect. 5.4, exactly solvable quantum systems with explicitly time-dependent interaction potentials are extremely rare. As demonstrated with (5.83), this is true already for the periodically driven two-level-system in a linearly polarized monochromatic field [11] for which no exact closed form solution can be found. Thus, we generally have to invoke numerical procedures.

5.5.1 Method of Floquet matrix

Since the Hamiltonian $H(x,t)$ and the Floquet modes are time-periodic, we can expand the Floquet solutions into the Fourier vectors $|n\rangle$, $n = 0, \pm 1, \pm 2, \ldots$, such that $\langle t|n\rangle = \exp(\mathrm{i}n\omega t)$,

$$\Phi_\alpha(x,t) = \sum_{n=-\infty}^{\infty} c_\alpha^n(x) \exp(\mathrm{i}n\omega t). \tag{5.116}$$

The functions $c_\alpha^n(x)$ can be expanded in terms of a complete orthonormal set $\{\varphi_k(x), k = 1, \ldots, \infty\}$, yielding in terms of the unperturbed eigenfunctions of $H_0(x)$,

$$\Phi_\alpha(x,t) = \sum_{k=1}^{\infty} \sum_{n=-\infty}^{\infty} c_{\alpha,k}^n \varphi_k(x) \exp(\mathrm{i}n\omega t), \tag{5.117}$$

with $c_{\alpha,k}^n = \langle \varphi_k | c_\alpha^n \rangle$. Hence, in terms of the kets $|\varphi_k\rangle$, $\langle x|\varphi_k\rangle = \varphi_k(x)$, the Floquet equation (5.14) reads

$$\sum_{k=1}^{\infty} \sum_{n=-\infty}^{\infty} \mathcal{H} c_{\alpha,k}^n |\varphi_k\rangle \exp(\mathrm{i}n\omega t) = \sum_{k=1}^{\infty} \sum_{n=-\infty}^{\infty} \epsilon_\alpha c_{\alpha,k}^n |\varphi_k\rangle \exp(\mathrm{i}n\omega t). \tag{5.118}$$

Setting $\langle \varphi_k | \langle m| \equiv \langle \varphi_k m|$ and multiplying (5.118) with $\langle \varphi_j m| \exp(-\mathrm{i}m\omega t)$ from the left, yields after a time-average over one period of driving, the system of equations

$$\sum_{n=-\infty}^{\infty} \sum_{k=1}^{\infty} \langle\langle \varphi_j m|\mathcal{H}|\varphi_k n\rangle\rangle c_{\alpha,k}^n = \epsilon_\alpha c_{\alpha,j}^m. \tag{5.119}$$

Here we used the scalar-product notation in (5.19). With the definition

$$H^{m-n} = \frac{1}{T} \int_0^T \mathrm{d}t\, H(t) \exp[-\mathrm{i}(m-n)\omega t], \tag{5.120}$$

one finds the Floquet-matrix representation for (5.119),

$$\sum_{k=1}^{\infty} \sum_{n=-\infty}^{\infty} \langle\langle \varphi_j m|\mathcal{H}_\mathrm{F}|\varphi_k n\rangle\rangle c_{\alpha,k}^n = \epsilon_\alpha c_{\alpha,j}^m, \tag{5.121}$$

with the Floquet matrix defined by

$$\langle\langle \varphi_j m|\mathcal{H}_\mathrm{F}|\varphi_k n\rangle\rangle \equiv \langle \varphi_j|H^{m-n}|\varphi_k\rangle + n\hbar\omega\delta_{n,m}\delta_{j,k}. \tag{5.122}$$

For a sinusoidal perturbation $H(t) = H_0 - 2\hbar\lambda x \sin(\omega t + \phi)$, the operator H^{m-n} takes on a triangular structure

$$H^{m-n} = H_0\delta_{m,n} + \mathrm{i}\hbar\lambda x\Big(\delta_{m,n+1}\exp(\mathrm{i}\phi) - \delta_{m,n-1}\exp(-\mathrm{i}\phi)\Big). \tag{5.123}$$

Hence, the operator $\mathcal{H}_\mathrm{F}$ has a block-triagonal structure with only the number of angular frequencies ω in the diagonal elements varying from block to block.

The quasienergies $\{\epsilon_\alpha\}$are now obtained as the eigenvalues of the secular equation

$$\det|\mathcal{H}_\mathrm{F} - \epsilon\mathbf{1}| = 0, \tag{5.124}$$

whose block-tridiagonal form provides the quasienergies $\{\epsilon_{\alpha,n}\}$ and eigenvectors $|\epsilon_{\alpha,n}\rangle$, obeying the periodicity properties

$$\epsilon_{\alpha,k} = \epsilon_{\alpha,0} + k\hbar\omega, \tag{5.125}$$

$$\langle\alpha, n+k|\epsilon_{\beta,m+k}\rangle = \langle\alpha, n|\epsilon_{\beta,m}\rangle. \tag{5.126}$$

From these solutions, the spectral decomposition in (5.33) and expressions for transition amplitudes can readily be derived.

Because the origin of time can be chosen arbitrarily, the quasienergies do not depend on the phase ϕ. In contrast however, the Floquet modes $\Phi(x,t;\phi)$ depend on the phase. Keeping the time t fixed the variation of ϕ over the interval of 2π allows to cover the time-dependence of the Floquet mode over a whole period T.

5.5.2 Matrix-continued-fraction method

The block-tridiagonal structure of the Floquet matrix can be used to implement an efficient numerical algorithm, termed matrix continued fraction (MCF) method. Our starting point is (5.121). Performing the sum over n one finds

$$\begin{aligned}(\epsilon_\alpha - m\hbar\omega)c^m_{\alpha,j} = \sum_{k=0}^{\infty}\Big[&c^m_{\alpha,k}\langle\varphi_j|H_0|\varphi_k\rangle - \mathrm{i}\hbar\lambda\exp(-\mathrm{i}\phi)c^{m+1}_{\alpha,k}\langle\varphi_j|x|\varphi_k\rangle \\ &+\mathrm{i}\hbar\lambda\exp(-\mathrm{i}\phi)c^{m-1}_{\alpha,k}\langle\varphi_j|x|\varphi_k\rangle\Big].\end{aligned} \tag{5.127}$$

This form can be cast into a tridiagonal recursive relation that reads

$$G(m,\alpha)c^m_\alpha + H^+c^{m+1}_\alpha + H^-c^{m-1}_\alpha = 0, \tag{5.128}$$

where

$$G(m,\alpha) = H_0 - (\epsilon_\alpha - m\hbar\omega)\mathbf{1} \tag{5.129}$$

and

$$H^\pm = \mp\mathrm{i}\hbar\lambda\exp(\mp\mathrm{i}\phi)x. \tag{5.130}$$

The recursive matrix equation in (5.128) can be solved by using the ladder operators

$$S_m c_\alpha^m = c_\alpha^{m+1},$$
$$T_{-m} c_\alpha^{-m} = c_\alpha^{-(m+1)}, \tag{5.131}$$

which are rising (lowering) the index m. The solutions of (5.131) can be given in terms of a matrix continued fraction, by iterating the recursive solution with m increasing,

$$\begin{aligned} S_{m-1} &= -[G(m,\alpha) + H^+ S_m]^{-1} H^- \\ &= -\frac{1}{G(m,\alpha) - H^+ \dfrac{1}{G(m+1,\alpha) - H^+ \ldots} H^-} H^-, \\ T_{-(m-1)} &= -[G(-m,\alpha) + H^- T_{-m}]^{-1} H^+ \\ &= -\frac{1}{G(-m,\alpha) - H^- \dfrac{1}{G(-m-1,\alpha) - H^- \ldots} H^+} H^+. \end{aligned} \tag{5.132}$$

Setting $m = 0$ yields from (5.128) the linear system of equations

$$G(0,\alpha) c_\alpha^0 + H^+ S_0 c_\alpha^0 + H^- T_0 c_\alpha^0 = 0, \tag{5.133}$$

composed of both diagonal and — via S_0, T_0 — also nondiagonal contributions. The quasienergies follow from the solubility condition,

$$\det[G(0,\alpha) + H^+ S_0 + H^- T_0] = 0. \tag{5.134}$$

In practice, this system of equations is solved numerically, by evaluating S_0 and T_0 truncated at some finite value $m > 0$, i.e. one assumes $S_m = 0$, $T_{-m} = 0$ for sufficiently large m, such that the result no longer changes significantly with increasing m. For an application of this MCF method to the problem of driven tunneling we refer the reader to the original literature [19].

The above two sections discussed the case of periodic perturbations. A general time-dependent interaction can be treated similarly — see Sect. 5.3 — by use of the multimode Floquet theory, or the general (t,t')-formalism with the time interval T being chosen sufficiently large. Time-periodic boundary conditions can usually be assumed for finite (laser-)pulse interactions also, when the number of oscillations during the pulse lifetime is large. Alternatively, various direct methods for solving a time-dependent quantum problem exist. It should be stressed again, that an avoidance of the time-ordering operator — via embedding (cf. Sect. 5.3) — results in a great simplification. Otherwise, the propagator must be split into short segments in which the Hamiltonian does not change significantly. Some keywords relating to these alternative direct time-propagation methods are the "split-operator technique" [20], and the "second-order-difference schemes". For recent surveys we refer the reader to the reviews in Ref. [21].

5.6 Coherent tunneling in driven bistable systems

In this section we address the physics of coherent transport in bistable systems. These systems are abundant in the chemical and physical sciences. On a quantum mechanical level of description, bistable, or double-well potentials, are associated with a paradigmatic coherence effect, namely quantum tunneling. Here we shall investigate the influence of a spatially homogeneous monochromatic driving on the quantal dynamics in a symmetric, quartic double well. This archetype system is particularly promising for studying the interplay between classical nonlinearity — its classical dynamics exhibits chaotic solutions — and quantum coherence. Its Hamiltonian reads [9, 19]

$$H(x,p;t) = \frac{p^2}{2m} + V_0(x) + xS\sin(\omega t + \phi), \tag{5.135}$$

with the quartic double well potentail

$$V_0(x) = -\frac{m\omega_0^2}{4}x^2 + \frac{m^2\omega_0^4}{64E_\mathrm{B}}x^4. \tag{5.136}$$

Here m denotes the mass of the particle, ω_0 is the classical frequency at the bottom of each well and E_B the barrier height, and S and ω are the amplitude and angular frequency of the driving. The number of doublets with energies below the barrier top is approximately given by $D = E_\mathrm{B}/\hbar\omega_0$. The classical limit hence amounts to $D \to \infty$.

For ease of notation, we introduce the dimensionless variables

$$\bar{x} = \sqrt{\frac{m\omega_0}{\hbar}}x, \tag{5.137}$$

$$\bar{p} = \frac{p}{\sqrt{m\omega_0\hbar}}, \tag{5.138}$$

$$\bar{t} = \omega_0 t, \tag{5.139}$$

$$\bar{\omega} = \frac{\omega}{\omega_0}, \tag{5.140}$$

$$\bar{S} = \frac{S}{\sqrt{m\omega_0^3\hbar}}, \tag{5.141}$$

where the overbar is omitted in the following. This is equivalent to setting formally $m = \hbar = \omega_0 = 1$.

As discussed in Section 5.3, the symmetry of $H(t)$ reflects a discrete translation symmetry in multiples of the external driving period $T = 2\pi/\omega$, i.e., $t \to t + nT$. Hence the Floquet operator describes the stroboscopic quantum propagation

$$K(nT,0) = [K(T,0)]^n. \tag{5.142}$$

Besides the invariance under discrete time translations, the periodically driven symmetric system exhibits a generalized parity symmetry P,

$$P : x \to -x; \qquad t \to t + T/2. \tag{5.143}$$

This generalized parity can be looked upon as an ordinary parity symmetry in the composite Hilbert space, $\mathcal{R} \otimes \mathcal{T}$. Just as in the unperturbed case with $S = 0$, this allows the classification of the corresponding quasienergies $\epsilon_{\alpha n}$ into an even and an odd subset. For very weak fields $S \to 0$, the quasienergies $\epsilon_{\alpha k}$ follow from (5.32) as

$$\epsilon^0_{\alpha k}(S, \omega) = E_\alpha + k\hbar\omega; \qquad k = 0, \pm 1, \pm 2, \ldots, \tag{5.144}$$

with $\{E_\alpha\}$ being the unperturbed eigenvalues in the symmetric double well. As pointed out in (5.16), this infinite multiplicity is a consequence of the fact that there are infinitly many possibilities to construct equivalent Floquet modes, cf. (5.15): The multiplicity is lifted if we consider the cyclic quasienergies mod $\hbar\omega$. Given a pair of quasienergies $\epsilon_{\alpha,k}$, $\epsilon_{\alpha',k'}$, $\alpha \neq \alpha'$, a physical significance can be attributed to the difference $\Delta k = k' - k$. For example, a crossing $\epsilon_{\alpha,k} = \epsilon_{\alpha',k+\Delta k}$ can be interpreted as a (Δk)-photon transition. With $S > 0$, the equality in (5.144) no longer provides a satisfactory approximation. Nevertheless, the driving field is still most strongly felt near the resonances $\epsilon_{\alpha,k} \approx \epsilon_{\alpha',k'}$. The physics of periodically driven tunneling can be qualified by the following two properties:

(i) First we observe, by an argument going back to von Neumann and Wigner [16], that two parameters must be varied independently to locate an accidental energy degeneracy. In other words, exact quasienergy crossings are found at most at isolated points in the parameter plane (S, ω), i.e., the quasienergies exhibit typically avoided crossings. In presence of the generalized parity symmetry in (5.143) in the extended space $\mathcal{R} \otimes \mathcal{T}$, however, this is true only among states belonging to the same parity class, or for cases of driven tunneling in presence of an asymmetry (then (5.143) no longer holds). With the symmetry in (5.143) present, however, quasienergies associated with eigenstates of opposite parity do exhibit exact crossings and form a one-dimensional manifold in the (S, ω)-plane, i.e., $\{\epsilon(S, \omega)\}$ exhibit an exact crossing along lines. With $S \to -S$, implying $\epsilon(S, \omega) = \epsilon(-S, \omega)$, these lines are symmetric around the ω-axis.

(ii) Second, the effective coupling due to the finite driving between two unperturbed levels at the crossing $E_\alpha = E_{\alpha'} - \Delta k\omega$, as reflected in the degree of splitting of that crossing at $S \neq 0$, rapidly decreases with increasing Δk, proportional to the power law $S^{\Delta k}$. This suggests the interpretation as a (Δk)-photon transition. Indeed, this fact can readily be substantiated by applying the usual (Δk)-th order perturbation theory. As a consequence, for small driving S only transitions with Δk a small whole number do exhibit a significant splitting.

5.6.1 Limits of slow and fast driving

In the limits of both slow (adiabatic) and fast driving we have a clearcut separation of time scales between the inherent tunneling dynamics and the external periodic driving. Hence, the two processes effectively uncouple and driven tunneling results in a mere renormalization of the bare tunnel splitting Δ. This result can be substantiated by explicit analytical calculations [19]. Let us briefly address the adiabatic limit, i.e., the driving frequency ω satisfies $\omega \ll \Delta$. Setting $\widetilde{\phi} \equiv (\omega t + \phi)$, the tunneling proceeds in the adiabatic potential

$$V(x, \widetilde{\phi}) = V_0(x) + xS \sin \widetilde{\phi}. \tag{5.145}$$

The use of the quantum adiabatic theorem predicts that $\Psi(x,t)$ will cling to the same instantaneous eigenstates. Thus, the evaluation of the periodic-driving renormalized tunnel splitting follows the reasoning used for studying the bare tunnel splitting in presence of an asymmetry σ,

$$\sigma = V(x_-, \widetilde{\phi}) - V(x_+, \widetilde{\phi}), \tag{5.146}$$

with $x_\pm$ denoting the two symmetric unperturbed metastable states. With the instantaneous splitting determined by $\Delta_\sigma = (\Delta^2 + \sigma^2)^{1/2}$, the averaging over the phase $\widetilde{\phi}$ between $[0, 2\pi]$ yields for the renormalized tunnel splitting $\Delta_{\rm ad}(S)$, the result [19]

$$\Delta_{\rm ad}(S) = (2\Delta/\pi)(1+\alpha)^{1/2} E\left[\sqrt{\alpha/(1+\alpha)}\right] \geq \Delta, \tag{5.147}$$

with $\alpha = 32S^2D/\Delta^2$, and $E[x]$ denoting the complete elliptical integral. This shows that $\Delta_{\rm ad}$ increases proportional to S^2 as $\alpha \ll 1$, and is increasing proportional to S for $\alpha \gg 1$. Hence, a particle localized in one of the two metastable states will not stay localized there (this would be the prediction based on the classical adiabatic theorem) but rather will tunnel forth and back with an increased tunneling frequency $\omega_{\rm ad} = \Delta_{\rm ad} > \Delta$. Obviously, with the slowly changing quantum system passing a near degeneracy (tunnel splitting), the limits $\hbar \to 0$, ω fixed and small (classical adiabatic theorem) and $\omega \to 0$, $\hbar$ fixed (quantum adiabatic theorem) are not equivalent.

The limit of high frequency driving can be treated analytically as well. The unitary transformation

$$\Psi(x,t) = \exp\left(-\mathrm{i}\frac{S}{\omega}\cos(\omega t + \phi)x\right) g(x,t) \tag{5.148}$$

describes the quantum dynamics within the familiar momentum coupling in terms of an electromagnetic potential $A(t) = -(S/\omega)\cos(\omega t + \phi)$, the transformed Hamiltonian reads

$$\widetilde{H}(x,t) = H_0(x,p) - A(t)p, \tag{5.149}$$

where we have dropped all time-dependent contributions that do not depend on x and p. Next we remove this $A(t)p$-term by a Kramers-Henneberger transformation,

$$g(x,t) = \exp\left(-\mathrm{i}\int^t \mathrm{d}t' A(t')p\right) f(x,t) \tag{5.150}$$

to yield

$$\widehat{H}(x,t) = \frac{1}{2}p^2 + V_0\left(x - \frac{S}{\omega^2}\sin(\omega t + \phi)\right), \tag{5.151}$$

resulting in a removal of the $A(t)p$-term, and the time-dependence shifted into the potential $V(x,t)$. After averaging over a cycle of the periodic perturbation we obtain an effective Hamiltonian

$$H_{\rm hf} = \frac{1}{2}p^2 - \frac{1}{4}x^2\left[1 - \frac{3}{16D}\left(\frac{S}{\omega^2}\right)^2\right] + \frac{1}{64D}x^4, \tag{5.152}$$

with a frequency-dependent curvature. This large-frequency approximation results in a high-frequency renormalized tunnel splitting [19],

$$\Delta_{\rm hf}/\Delta = \left(1 - \frac{3}{16D}\left(\frac{S}{\omega^2}\right)^2\right)\exp\left(\frac{2S^2}{\omega^4}\right) \geq 1. \tag{5.153}$$

Hence, fast driving results in an effective reduction of barrier height, thereby increasing the net tunneling rate. In conclusion, the regime of adiabatic slow driving and very-high-frequency driving (away from high-order resonance) can be modeled via a driving-induced enhancement of the tunnel splitting. A similar shortening of the effective tunneling duration $\tau_{\rm T} \equiv \pi/\Delta$ can be achieved alternatively with an appropriate shaping of the perturbation amplitude; $S \to S(t) = S\sin^2(\pi t/t_{\rm p})$, with $t_{\rm p}$ being the pulse duration [32].

5.6.2 Driven tunneling near a resonance

Qualitative changes of the tunneling behavior are expected as soon as the driving frequency becomes comparable to internal resonance frequencies of the unperturbed double well with energy eigenstates E_1, $E_2, \ldots$ with corresponding eigenfunctions $\varphi_1(x)$, $\varphi_2(x), \ldots$ Thus, such resonances occur at $\omega = E_3 - E_2$, $E_4 - E_1$, $E_5 - E_2$, ... etc. A spectral decomposition of the dynamics resolves the temporal complexity which is related to the landscape of quasienergies planes $\epsilon_{\alpha,k}(S,\omega)$ in parameter space. Most important are the features near close encounters among the quasienergies. In particular, two quasienergies can cross one another if they belong to different parity classes, or otherwise, they form an avoided crossing. The situation for a single-photon transition-induced tunneling is depicted in Fig. 5.3 at the fundamental resonance $\omega = E_3 - E_2$. For $S > 0$, the corresponding quasienergies ϵ_{2k} and $\epsilon_{3,k-1}$ form avoided crossings, because they possess equal parity quantum numbers. Starting from a state localized in the left well, we depict in Fig. 5.3a the probability to return $P^{\Psi}(t_n) = |\langle\Psi(0)|\Psi(t_n)\rangle|^2$, $t_n = nT$. Instead of a monochromatic oscillation, which characterizes the unperturbed tunneling we observe in the driven case a complex beat pattern. Its Fourier transform reveals that it is mainly composed of two groups of three frequencies each (Fig. 5.3b). These beat frequencies can be associated with transitions among Floquet states at the avoided crossing pertaining to the two lowest doublets. The lower triplet is made up of the quasienergy differences $\epsilon_{3,-1} - \epsilon_{2,0}$, $\epsilon_{2,0} - \epsilon_{1,0}$, $\epsilon_{3-1} - \epsilon_{1,0}$; the higher triplet is

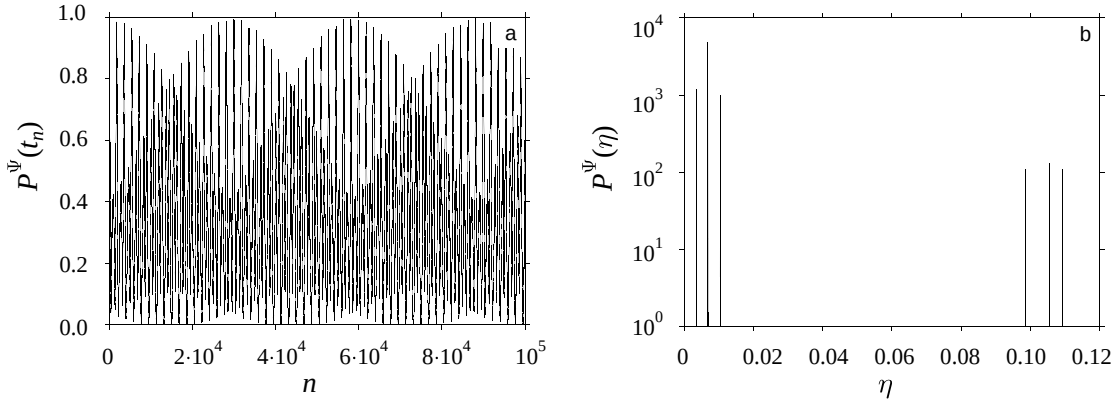

Fig. 5.3: Driven tunneling at the fundamental resonance, $\omega = E_3 - E_2$. (a) Time evolution of $P^{\Psi}(t_n)$ over the first 10^5 time steps; (b) corresponding local spectral two-point correlations $P_2^{\Psi}(\eta)$ [19]. The parameter values are $D = 2, S = 2 \times 10^{-3}$, and $\omega = 0.876$.

composed of the differences $\epsilon_{4,-1} - \epsilon_{3,-1}$, $\epsilon_{4,-1} - \epsilon_{2,0}$, $\epsilon_{4,-1} - \epsilon_{1,0}$ [19]. An analytical, weak-field and weak-coupling treatment of a resonantly driven two-doublet system has been presented with Refs. [33, 34].

5.6.3 Coherent destruction of tunneling

A particularly interesting phenomenon occurs if we focus on near-degenerate states that are tunnel splitted. For example, in the deep quantum regime the two quasienergies $E_1 \to \epsilon_{1k}(S, \omega)$ and $E_2 \to \epsilon_{2k}(S, \omega)$ the subsets $\{\epsilon_{1,k+1}(S, \omega\}$ and $\{\epsilon_{2,k-1}(S, \omega)\}$ belong to different parity classes so that they can form exact crossings on one-dimensional manifolds, see below (5.144); put differently, at the crossing the corresponding two-photon transition that bridges the unperturbed tunnel splitting Δ is parity forbidden. To give an impression of driven tunneling in the deep quantal regime, we study how a state, prepared as a localized state centered in the left well, evolves in time under the external force. Since this state is approximately given by a superposition of the two lowest unperturbed eigenstates, $|\Psi(0)\rangle \approx (|\Psi_1\rangle + |\Psi_2\rangle)/\sqrt{2}$, its time evolution is dominated by the Floquet-state doublet originating from $|\Psi_1\rangle$ and $|\Psi_2\rangle$, and the splitting $\epsilon_2 - \epsilon_1$ of its quasienergies. Then a vanishing of the difference $\epsilon_{2,-1} - \epsilon_{1,1}$ does have an intriguing consequence: For an initial state prepared exactly as a superposition of the corresponding two Floquet states $\Psi_{1,1}(x, t)$ and $\Psi_{2,-1}(x, t)$, cf. (5.11), (5.15), the probability to return $P(t_n)$, probed at multiples of the fundamental driving period $T = 2\pi/\omega$, becomes time independent. This gives us the possibility that tunneling can be brought to a complete standstill [9, 19]. For this to happen, it is necessary that the particle does not spread and/or tunnel back and forth during a full cycle of the external period T after which the two Floquet modes assemble again [35]. Hence, this condition [9, 35], together with the necessary condition of exact crossing between the tunneling related quasienergies $\epsilon_{2n,k-1} = \epsilon_{2n-1,k+1}$, ($n$: number of tunnel-splitted dublett) guarantees that tunneling can be brought to a complete standstill in a dynamically

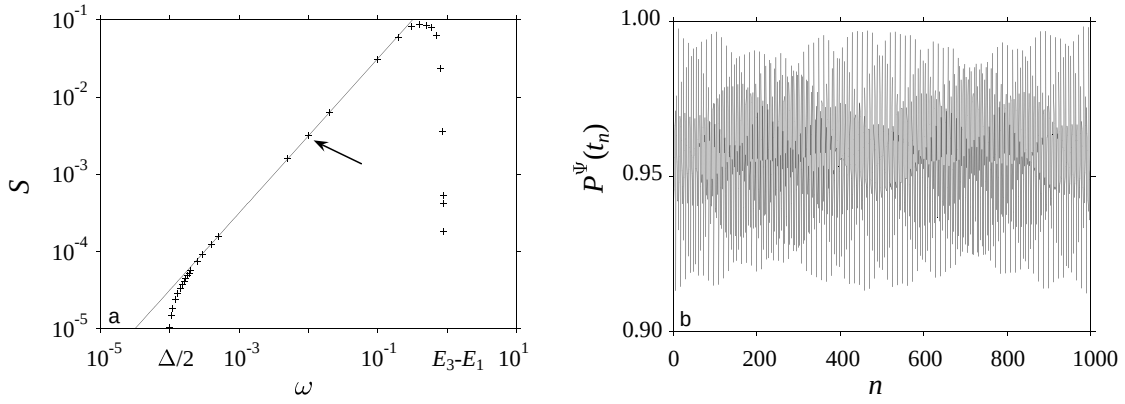

Fig. 5.4: Suppression of tunneling at an exact crossing, $\epsilon_{2,-1} = \epsilon_{1,1}$. (a) One of the manifolds in the (S, ω)-plane where this crossing occurs (data obtained by diagonalization of the full Floquet operator for the driven double well are indicated by crosses, the full line has been derived from a two-state approximation, the arrow indicates the parameter pair for which part (b) of this figure has been obtained); (b) time evolution of $P^{\Psi}(t_n)$ over the first 1000 time steps, starting from an initial state prepared as a coherent state in the left well.

coherent manner. In Fig. 5.4a we depict the corresponding one-dimensional manifold of the j-th crossing between the quasienergies that relate to the lowest tunnel dublett, i.e., $M^{j=1}_{\rm loc}(S, \omega)$, which is a closed curve that is reflection symmetric with respect to the line $S = 0$, there a localization of the wave function $\Psi(x, t)$ can occur. A typical time evolution of $P(t_n)$ for a point on the linear part of that manifold is depicted in panel 4b.

Moreover, a time-resolved study over a full cycle (not depicted) does indeed show that the particle stays localized also at times $t \neq t_n$. Almost complete destruction of tunneling is found to occur on $M^1_{\rm loc}$ for $\Delta < \omega < E_3 - E_2$. For $\omega \to E_3 - E_2$, the strong participation of a third quasienergy mixes nonzero frequencies into the time dependence so that coherent destruction of tunneling at all times ceases to exist. For small frequencies, $\Delta/2 \leq \omega \leq \Delta$, and corresponding small driving strengths S, as implied by $M^1_{\rm loc}(S, \omega)$, the driven quantum mechanics approaches the unperturbed quantum dynamics. In particular, it follows from (5.31), (5.32) for $\omega \to \Delta/2$ and $S \to 0$, $\Phi_{1,1}(x, t) = \varphi_1(x) \exp(\mathrm{i}\omega t)$, $\Phi_{2,-1}(x, t) = \varphi_2(x) \exp(-\mathrm{i}\omega t)$, that

$$P(t) = |\langle \Psi(0) | \Psi(t) \rangle|^2 = \cos^2(\Delta t/2), \qquad \omega = \Delta/2. \tag{5.154}$$

For $\omega \approx \Delta$, $\epsilon_{1,1}$ and $\epsilon_{2,-1}$ exhibit an exact crossing. With corresponding Floquet modes determined from perturbation theory as

$$\Phi_{1,1}(x, t) \sim \frac{1}{\sqrt{2}} [\varphi_1(x) \exp(\mathrm{i}\omega t) + \mathrm{i}\varphi_2(x)],$$

$$\Phi_{2,-1}(x, t) \sim \frac{1}{\sqrt{2}} [\varphi_2(x) \exp(-\mathrm{i}\omega t) + \mathrm{i}\varphi_1(x)], \tag{5.155}$$

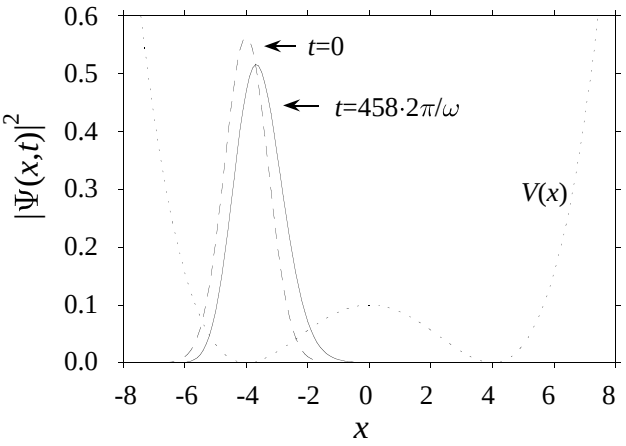

Fig. 5.5: The probability $|\langle\Psi(t)|x\rangle|^2$ at $t = 458\,T$ (full line) is compared with the initial state (dashed line, the dotted line depicts the unperturbed symmetric bistable potential). The parameters are $D = 2, S = 3.171 \times 10^{-3}$ and $\omega = 0.01$, i.e., ω equals 52.77 times the unperturbed tunnel splitting.

the result for $P(t)$, with $\Psi(x,0) = [\varphi_1(x)+\varphi_2(x)]/\sqrt{2}$, localized in the left well, becomes

$$P(t) \sim \frac{1}{4}[3 + \cos(2\Delta t)], \qquad \omega \approx \Delta. \tag{5.156}$$

For larger frequencies obeying $\Delta < \omega < E_3 - E_2$, the Floquet modes can be approximated by [35]

$$\begin{aligned} \Phi_{1,1}(x,t) &\sim \varphi_2(x)|\sin(\omega t)| - \mathrm{i}\varphi_1(x)\cos(\omega t), \\ \Phi_{2,-1}(x,t) &\sim \varphi_1(x)|\sin(\omega t)| - \mathrm{i}\varphi_2(x)\cos(\omega t). \end{aligned} \tag{5.157}$$

This results in a complete localization,

$$P(t) = 1, \qquad \Delta < \omega \leq E_3 - E_2. \tag{5.158}$$

Throughout Eqs. (5.154) — (5.158), we set the initial phase in (5.135) equal to zero.

Starting from a coherent state localized in the left well, taken as the ground state of the harmonic approximation, we depict in Fig. 5.5 the spatially resolved tunneling dynamics for $|\Psi(x,t)|^2$ at time $t = 0$ and at time $t = 458\,T$ for $\omega = 0.01 = 52.77\Delta$, and $S = 3.17 \times 10^{-3}$, yielding an exact crossing between $\epsilon_{1,1}$ and $\epsilon_{2,-1}$. For this value of $n = 458$, the deviation which originates from small admixtures of higher-lying quasienergy states to the initial coherent state, is exceptionally large. For other times the localization is even better. It is hence truly remarkable that the coherent destruction of tunneling on $M^1_{\rm loc}(S,\omega)$, with $\Delta < \omega < E_2 - E_1$, is essentially not affected by the intrinsic time dependence of the corresponding Floquet modes, nor by the presence of other quasienergy states $\epsilon_{\alpha,k}$, $\alpha = 3, 4, \ldots$.

5.6.4 Two-state approximation to driven tunneling

Additional insight into the mechanism of coherent destruction of tunneling can be obtained if one simplifies the situation by neglecting all of the spatial information contained in the Floquet modes $\Phi_\alpha(x,t)$ and restricting the influence of all quasienergies to the lowest doublet only [35–39]. Such a two-state approximation cannot reproduce those sections of the localization manifolds that are affected by resonances, e.g. the part in Fig. 5.3a that bends back to $S=0$ for $\omega < E_3 - E_2$. Setting for the transition dipole moment $S\langle\varphi_1|x|\varphi_2\rangle \equiv 2\lambda$, we find within the localized basis the TLS Hamiltonian in (5.91). For the state vector in this localized basis $|+\rangle$ and $|-\rangle$, we set

$$|\Psi(t)\rangle = c_1(t)\exp[-\mathrm{i}(2\lambda/\omega)\ \sin\omega t]|-\rangle$$
$$+c_2(t)\exp[+\mathrm{i}(2\lambda/\omega)\sin\omega t]|+\rangle. \tag{5.159}$$

Given the $\cos(\omega t)$ perturbation, $\phi = \pi/2$, we consequently obtain from the Schrödinger equation for the amplitudes $\{c_{1,2}(t)\}$ the equation

$$\mathrm{i}\frac{\mathrm{d}}{\mathrm{d}t}c_{1,2}(t) = -\frac{1}{2}\Delta\exp[\pm\mathrm{i}(4\lambda/\omega)\sin(\omega t)]c_{2,1}(t). \tag{5.160}$$

For large frequencies $\omega \gg \Delta$, we average (5.160) over a complete cycle to obtain the high-frequency approximation

$$\mathrm{i}\frac{\mathrm{d}}{\mathrm{d}t}c_{1,2}(t) = -\frac{1}{2}\Delta J_0(4\lambda/\omega)c_{2,1}(t), \tag{5.161}$$

where $J_0(x) = (\omega/2\pi)\int_0^T \mathrm{d}s\exp\left[\mathrm{i}x\sin(\omega s)\right]$, is the zeroth-order Bessel function of the first kind. This yields a static approximation — which is different from the RWA in (5.85) — with a frequency-renormalized splitting

$$\Delta \to J_0(4\lambda/\omega)\Delta. \tag{5.162}$$

The static TLS is easily solved to give with $c_1(t=0)=1$ for the return probability $P(t)$ the approximate result

$$P(t) = |c_1(t)|^2 = \cos^2\Big(J_0(4\lambda/\omega)\Delta t/2\Big). \tag{5.163}$$

On the localization manifold $M^1_{\mathrm{loc}}(\lambda,\omega)$, we find from (5.162) at the first zero of $J_0(x_1)=0$, i.e., $4\lambda/\omega = 2.40482\ldots$, in agreement with the result in (5.93). On this manifold, $P(t)$ in (5.163) precisely equals unity, i.e., the effective tunnel splitting vanishes. Thus one finds a complete coherent destruction of tunneling. This high-frequency TLS approximation, as determined by the first root of $J_0(4\lambda/\omega)$, is depicted in Fig. 5.4a by a solid line. Higher roots yield an approximation for M^j_{loc} with $j>1$. Moreover, we note that $J_0(x) \sim x^{-1/2}$ as $x\to\infty$. This implies, within the TLS-approximation to driven tunneling, that tunneling is always suppressed for $\omega > \Delta$ with $4\lambda/\omega \gg 1$. An improved formula for $P(t)$ in (5.163), that contains also higher

odd harmonics of the fundamental driving frequency ω has recently been given in [39]. This driven TLS is closely connected with the problem of periodic, nonadiabatic level crossing. In the diabatic limit $\delta \equiv \Delta^2/(\lambda\omega) \to 0$, corresponding to a large amplitude driving, the return probability has been evaluated by Kayanuma [38]. In our notation and with $\lambda > \max(\omega, \Delta)$ this result reads

$$P(t) \sim \cos^2\left(\left(\frac{\omega}{2\lambda\pi}\right)^{1/2}\left[\sin\left(\frac{4\lambda}{\omega}+\frac{\pi}{4}\right)\right]\frac{\Delta t}{2}\right). \tag{5.164}$$

With $J_0 \sim (2/\pi x)^{1/2}\sin(x+\pi/4)$, for $x \gg 1$, (5.164) reduces for $\lambda/\omega \gg 1$ to (5.163). Here, the phase factor of $\pi/4$ corresponds to the Stokes phase known from diabatic level crossing [38], and $4\lambda/\omega$ is the phase acquired during a single crossing of duration $T/2$. The mechanism of coherent destruction of tunneling in this limit $\lambda > \max(\omega, \Delta)$ hence is related to a destructive interference between transition paths with $4\lambda/\omega = n\pi + 3\pi/4$. The phenomenon of coherent destruction of tunneling also persists if we use a full quantum treatment for the semiclassical description of the field: For a quantized electromagnetic field $S \to (a^+ + a)$, the quantized version of (5.3) reads

$$H = -\frac{1}{2}\Delta\sigma_z + \omega a^+ a - g(a^+ + a)\sigma_x. \tag{5.165}$$

With $\langle n\rangle = \langle a^+ a\rangle$ the coupling constant g is related to the semiclassical field λ by

$$g\sqrt{n} = \lambda. \tag{5.166}$$

The vanishing of the quasienergy difference is then controlled by the roots of the Laguerre polynomial L_n of the order of the photon number n [40]. With a large photon number one recovers with $L_n \propto J_0$, as $n \gg 1$, the semiclassical description. Just as is the case with the semiclassical description, a rotating-wave approximation of the quantum TLS in (5.165), giving the celebrated Jaynes-Cummings model [41], is not able to reproduce the tunneling-suppression phenomenon.

5.7 Laser control of quantum dynamics

The previous phenomenon of coherent destruction of tunneling is an example of a dynamical quantum interference effect by which the quantum dynamics can be manipulated by an observer. More generally, the dependence of quasienergies on field strength and frequency can be used to control the emission spectrum by either generating or by selectively eliminating specific spectral lines. For example, the near crossing of quasienergies in a symmetric double well generates anomalous low-frequency lines and — at exact crossing — doublets of intense even-harmonic generation (EHG) [10]. This latter phenomenon is intriguing: A symmetric system possesses inversion symmetry so that even harmonics are forbidden by selection rules valid to all orders in perturbation theory. EHG thus precisely occurs at the exact crossings where tunneling can be frozen, so that a dynamically induced static dipole moment is generated.

This control by a periodic continuous-wave driving can be generalized by recourse to more complex perturbations. The goal by which a pre-assigned task for the output of a quantum dynamics is imposed from the outside by applying a sequence of properly designed (in phase and/or shape) pulse perturbations is known as quantum control [8]. For example, a primary goal in chemical physics is to produce desired product yields or to manipulate the atomic and molecular properties of matter [8, 42, 43]. As an archetype situation, we present the control of the quantum dynamics of two coupled electronic surfaces

$$\mathrm{i}\hbar\frac{\partial}{\partial t}\begin{pmatrix}\Psi_{\mathrm{g}}\\ \Psi_{\mathrm{e}}\end{pmatrix}=\begin{bmatrix}H_{\mathrm{g}} & -\mu(R)E(t)\\ -\mu(R)E^{*}(t) & H_{\mathrm{e}}\end{bmatrix}\begin{pmatrix}\Psi_{\mathrm{g}}\\ \Psi_{\mathrm{e}}\end{pmatrix}, \tag{5.167}$$

where R denotes the nuclear coordinates and $H_{\mathrm{g,e}}$ are the Born-Oppenheimer Hamiltonians for the ground- (g) and excited- (e) field free surfaces, respectively. The surfaces are coupled within the dipole approximation by the transition dipole operator $\mu(R)$ and the generally complex-valued radiation field $E(t)$. Notice that the structure in (5.167) is identical to that obtained in the driven TLS. Following Kosloff, Hammerich, and Tannor [43], the rate of change to the ground-state population $n_{\mathrm{g}}(t)=\langle\Psi_{\mathrm{g}}(t)|\Psi_{\mathrm{g}}(t)\rangle$ is readily evaluated to read

$$\begin{aligned}\frac{\mathrm{d}n_{\mathrm{g}}}{\mathrm{d}t}&=2\,\mathrm{Re}\langle\Psi_{\mathrm{g}}|\dot{\Psi}_{\mathrm{g}}\rangle\\ &=-\frac{2}{\hbar}\,\mathrm{Im}\Big(\langle\Psi_{\mathrm{g}}(t)|\mu(R)|\Psi_{\mathrm{e}}(t)\rangle E(t)\Big).\end{aligned} \tag{5.168}$$

If we set with $C(t)$ a real-valued function

$$E(t)\to E_0(t)=\langle\Psi_{\mathrm{e}}(t)|\mu(R)|\Psi_{\mathrm{g}}(t)\rangle C(t), \tag{5.169}$$

we can freeze the population transfer (null-population transfer), with (5.169),

$$\frac{\mathrm{d}n_{\mathrm{g}}}{\mathrm{d}t}=0, \tag{5.170}$$

for all times t. In other words, the population in the ground electronic surface, and necessarily also the population of the excited surface, remains fixed. If we were to chose $E(t)\to\mathrm{i}E_0(t)$, it would cause population to be transferred to the upper state, while $E(t)\to-\mathrm{i}E_0(t)$ would dump population down to the groundstate. Hence, by controlling the phase of a laser, we can control the population transfer at will. This phenomenon applies equally well to driven tunneling in a TLS. What can we achieve if we manipulate the amplitude $C(t)$? The change in the energy of the ground state surface, which can be varied by exciting specific ground-state vibrational modes, is obtained as

$$\frac{\mathrm{d}E_{\mathrm{g}}}{\mathrm{d}t}=\frac{\mathrm{d}}{\mathrm{d}t}\frac{\langle\Psi_{\mathrm{g}}(t)|H_{\mathrm{g}}|\Psi_{\mathrm{g}}(t)\rangle}{\langle\Psi_{\mathrm{g}}(t)|\Psi_{\mathrm{g}}(t)\rangle}. \tag{5.171}$$

Under the null-population-transfer condition in (5.169), this simplifies to [43]

$$\frac{\mathrm{d}E_{\mathrm{g}}}{\mathrm{d}t} = -\frac{2C(t)}{\hbar n_{\mathrm{g}}} \operatorname{Im} \langle \Psi_{\mathrm{g}}(t)|H_{\mathrm{g}}\mu(R)|\Psi_{\mathrm{e}}(t)\rangle\langle\Psi_{\mathrm{e}}(t)|\mu(R)|\Psi_{\mathrm{g}}(t)\rangle. \tag{5.172}$$

It follows that the sign of $C(t)$ can be used to "heat" or "cool" the ground-state wavepacket; the magnitude of $C(t)$ in turn controls the rate of heating (or cooling). With this scheme of phase and amplitude control of a laser pulse it is possible to excite vibrationally the lower state surface while minimizing radiation damage either by ionizing or by dissociating the corresponding quantum system.

5.8 Conclusions and outlook

In this chapter we presented a "tour of horizon" of the physics occurring in driven quantum systems. The use and advantages of the Floquet-theoretical method and its generalizations have been discussed. In particular, these methods provide a consistent physical picture for intensity-dependent nonlinear quantum phenomena in terms of Floquet modes and energy scales, as determined by corresponding quasienergy differences. Not surprisingly, exactly solvable quantum problems with time-dependent potentials are quite rare, Sect. 5.4. The Floquet method can be implemented rather effectively in numerical calculation schemes, cf. Sect. 5.5, and, most importantly, they are non-perturbative in nature, applicable to arbitrarily strong fields beyond the conventional rotating-wave schemes. Its use in driven quantum systems results in new phenomena such as frequency-shifts of resonances (Bloch-Siegert shifts), multi-photon transitions, the result of coherent destruction of tunneling [9, 19] and related, the generation of low-frequency radiation and intense even-harmonic generation. Finally, we discussed the application of non-periodic, pulse-designed perturbations to control — a priori — quantum properties such as the population transfer and reaction yields in laser driven quantum processes.

Several topics remained untouched. For example, we mainly restricted the discussion to bound quantum states, to problems with a pure point spectrum for the quasienergies. Interesting problems occur, however, also for driven quantum transport that involves scattering states. Such examples are the quenching of transmission in potential driven resonant tunneling diodes [44], or the driven quantum transport in a periodic tight binding model [45, 46]. In situations where unbound quantum states determine the physics (ionization, dissociation, decay of resonances, ac-driven tunneling decay, etc.), it is necessary to rotate the coordinates of the Hamiltonian into the complex plane (complex scaling) [47]. This procedure results in complex-valued quasienergies. For applications we refer the reader to the references given in [47]. Moreover, the problem of the effect of weak or even strong dissipation on the coherent dynamics of driven systems was also not touched upon. The topic of quantum dissipation, see chapter 4, extended to driven systems, is a nontrivial task. Now the bath modes couple resonantly to differences of quasienergies rather than to unperturbed energy differences with the latter being of relevance when the time-dependent

interaction is switched off. Consistent quantitative treatments of dissipation for driven quantum systems are difficult, but represent a challenging area of timely research. First interesting accomplishments have been put forward recently in Ref. [48]. Strong driving and moderate-to-strong dissipation are of particular importance for the intriguing phenomenon of nonlinear Quantum Stochastic Resonance [49]. Also, we have mainly addressed the driven dynamics in the deep quantum regime. Characteristic for driven quantum systems is that these exhibit a chaotic dynamics in the classical limit. For the phenomena occurring near the border line between quantum and classical dynamics, where a full semiclassical description is appropriate, the reader is refered to chapter 6 on quantum chaos. With driven quantum systems containing a rich repertory for novel phenomena, and providing us with the tool to control selectively the quantum dynamics, we hope that the readers become invigorated to extend and enrich the physics of strongly driven quantum systems with own original contributions.

References

[1] N. L. Manakov, V. D. Ovsiannikov, and L. P. Rapoport, Phys. Rep. **141**, 319 (1986).

[2] S.-I. Chu, Adv. Chem. Phys. **73**, 739 (1986).

[3] G. Casati and L. Molinari, Progr. Theor. Phys. Suppl. **98**, 287 (1989).

[4] A. G. Fainshtein, N. L. Manakov, V. D. Ovsiannikov, and L. P. Rapoport, Phys. Rep. **210**, 111 (1992).

[5] H. R. Reiss, Phys. Rev. Lett. **25**, 1149 (1970).

[6] M. Gavrila and J. Z. Kaminski, Phys. Rev. **52**, 613 (1984);
Q. Su and J. H. Eberly, Phys. Rev. A **44**, 5997 (1991);
F. Bensch, H. J. Korsch and N. Moiseyev, Phys. Rev. A **43**, 5145 (1991);
H. Wiedemann, J. Mostowski, and F. Haake, Phys. Rev. A **49**, 1171 (1994).

[7] For reviews see:
G. Casati, I. Guarneri, D. L. Shepelyansky, IEEE J. Quant. Elect. **24**, 1420 (1988);
R. Shakeshaft, Comments At. Mol. Phys. **28**, 179 (1992);
Laser Phys. **3**, No. 2 (1993), special issue on *Atoms, Ions and Molecules in a Strong Laser Field*, edited by A. M. Prokhorov.

[8] D. J. Tannor and S. A. Rice, Adv. Chem. Phys. **70**, 441 (1988);
P. Brumer and M. Shapiro, Ann. Rev. Phys. Chem. **43**, 257 (1992);
D. J. Tannor, in: *Molecules and Laser Fields*, edited by A. D. Bardrak, (Dekker, 1993), pp. 403 - 446.

[9] F. Grossmann, T. Dittrich, P. Jung and P. Hänggi, Phys. Rev. Lett. **67**, 516 (1991);
for a review see: P. Hänggi, Control of Tunneling, in: *Quantum Dynamics of Submicron Structures*, edited by H. A. Cerdeira, B. Kramer and G. Schön, Vol. 291

of *NATO Advanced Study Institute Series E: Applied Sciences* (Kluwer Academic Publishers, Boston, 1995), pp. 673 - 686.

[10] R. Bavli and H. Metiu, Phys. Rev. A **47**, 3299 (1993);
Yu. Dakhnovskii and H. Metiu, Phys. Rev. A **48**, 2342 (1993).

[11] J. H. Shirley, Phys. Rev. **138**, B979 (1965).

[12] Ya. B. Zeldovitch, Sov. Phys. JETP **24**, 1006 (1967);
V. I. Ritus, Sov. Phys. JETP **24**, 1041 (1967).

[13] G. Floquet, Ann. de l'Ecole Norm. Sup. **12**, 47 (1883);
E. L. Ince, *Ordinary Diffential Equations* (Dover Publ., New York, 1956);
W. Magnus and S. Winkler, *Hill's Equation* (Dover Publ., New York, 1979).

[14] H. Sambe, Phys. Rev. A **7**, 2203 (1973).

[15] A. G. Fainshtein, N. L. Manakov, and L. P. Rapoport, J. Phys. B **11**, 2561 (1978).

[16] J. von Neumann and E. Wigner, Physik. Zeitschr. **30**, 467 (1929).

[17] F. Bloch and A. Siegert, Phys. Rev. **57**, 522 (1940).

[18] Ya. B. Zeldovitch, Usp. Fiz. Nauk. **110**, 139 (1973);
T.-S. Ho and S.-I. Chu, Chem. Phys. Lett. **141**, 313 (1987).

[19] F. Grossmann, P. Jung, T. Dittrich, and P. Hänggi, Z. Phys. B **84**, 315 (1991).

[20] M. D. Feit, J. A. Fleck Jr., and A. Steiger, J. Comput. Phys. **47**, 412 (1982).

[21] R. Kosloff and D. J. Kosloff, J. Comput. Phys. **63**, 363 (1986);
R. Kosloff, J. Phys. Chem. **92**, 2087 (1988).

[22] J. Howland, Math. Ann. **207**, 315 (1974).

[23] U. Peskin and N. Moiseyev, J. Chem. Phys. **99**, 4590 (1993);
P. Pfeifer and R. D. Levine, J. Chem. Phys. **79**, 5512 (1983);
N. Moiseyev, Comments At. Mol. Phys. **31**, 87 (1995).

[24] K. Husimi, Progr. Theor. Phys. **9**, 381 (1953);
see also F. H. Kerner, Can. J. Phys. **36**, 371 (1958).

[25] A. M. Perelomov and V. S. Popov, Teor. Mat. Fiz. **1**, 275 (1970) [Sov. Phys. JETP **30**, 910 (1970)].

[26] C. Zerbe and P. Hänggi, Phys. Rev. E **52**, 1533 (1995).

[27] D. R. Dion and J. Hirschfelder, Adv. Chem. Phys. **35**, 265 (1976);
P. K. Aravind and J. O. Hirschfelder, J. Phys. Chem. **88**, 4788 (1984).

[28] I. I. Rabi, Phys. Rev. **51**, 652 (1937);
see also the preceding work: J. Schwinger, Phys. Rev. **51**, 648 (1937).

[29] I. Zak, Phys. Rev. Lett. **71**, 2623 (1993).

[30] M. Holthaus, G. H. Ristow, and D. W. Hone, Europhys. Lett. **32**, 241 (1995).

[31] M. Wagner, Phys. Rev. Lett. **76**, 4010 (1996).

[32] M. Holthaus, Phys. Rev. Lett. **69**, 1596 (1992).

[33] J. M. Gomez Llorente and J. Plata, Phys. Rev. E **49**, 2759 (1994).

[34] P. Goetsch and R. Graham, Ann. Physik **1**, 662 (1992).

[35] F. Grossmann and P. Hänggi, Europhys. Lett. **18**, 571 (1992).

[36] J. M. Gomez Llorente and J. Plata, Phys. Rev. A **45**, R6958 (1992).

[37] L. Wang and J. Shao, Phys. Rev. A **49**, R 637 (1994).

[38] Y. Kayanuma, Phys. Rev. A **50**, 843 (1994).

[39] X. G. Zhao, Phys. Lett. A **193**, 5 (1994); cf. eq. (41) therein.

[40] J. Plata and J. M. Gomez Llorente, Phys. Rev. A **48** 782 (1993);
D. E. Makarov, Phys. Rev. E **48**, R4164 (1993);
P. Neu and R. J. Silbey, Phys. Rev. A, **54**, 5323 (1996).

[41] E. T. Jaynes and F. W. Cummings, Proc. IRE **51**, 89 (1963).

[42] D. J. Tannor, Nature **369**, 445 (1994).

[43] R. Kosloff, A. D. Hammerich and D. J. Tannor, Phys. Rev. Lett. **69**, 2172 (1992).

[44] M. Wagner, Phys. Rev. B **49**, 16544 (1994);
M. Wagner, Phys. Rev. A **51**, 798 (1995).

[45] D. H. Dunlap and V. M. Kenkre, Phys. Rev. B **34**, 3625 (1986);
D. H. Dunlap and V. M. Kenkre, Phys. Rev. B **37**, 6622 (1988).

[46] M. Holthaus, Z. Phys. B **89**, 251 (1992);
M. Holthaus, Phys. Rev. Lett. **69**, 351 (1992);
H. Yamada, K. Ikeda, and M. Goda, Phys. Lett. A **182**, 77 (1993);
J. Rotvig, A. Jauho, and H. Smith, Phys. Rev. Lett. **74**, 1831 (1995).

[47] Y.K. Ho, Phys. Rep. **99**, 1 (1983);
N. Moiseyev and H. J. Korsch, Phys. Rev. A **41**, 498 (1990);
F. Grossmann and P. Hänggi, Chem. Phys. **170**, 295 (1993);
F. Grossmann and P. Hänggi, Europhys. Lett. **18**, 1 (1992).

[48] T. Dittrich, B. Oelschlägel, and P. Hänggi, Europhys. Lett. **22**, 5 (1993);
Yu. Dakhnovskii, Ann. Phys. (N.Y.) **230**, 145 (1994);
M. Grifoni, M. Sassetti, P. Hänggi, and U. Weiss, Phys. Rev. E **52**, 3596 (1995).

[49] M. Grifoni and P. Hänggi, Phys. Rev. Lett. **76**, 1611 (1996);
M. Grifoni and P. Hänggi, Phys. Rev. E **54**, 1390 (1996).